Spring 2015

High frequency field potentials of the cerebellar cortex

Jonathan David Groth
New Jersey Institute of Technology

Copyright Warning & Restrictions

The copyright law of the United States (Title 17, United States Code) governs the making of photocopies or other reproductions of copyrighted material.

Under certain conditions specified in the law, libraries and archives are authorized to furnish a photocopy or other reproduction. One of these specified conditions is that the photocopy or reproduction is not to be "used for any purpose other than private study, scholarship, or research." If a, user makes a request for, or later uses, a photocopy or reproduction for purposes in excess of "fair use" that user may be liable for copyright infringement,

This institution reserves the right to refuse to accept a copying order if, in its judgment, fulfillment of the order would involve violation of copyright law.

Please Note: The author retains the copyright while the New Jersey Institute of Technology reserves the right to distribute this thesis or dissertation

Printing note: If you do not wish to print this page, then select "Pages from: first page # to: last page #" on the print dialog screen

ABSTRACT

HIGH FREQUENCY FIELD POTENTIALS OF THE CEREBELLAR CORTEX

by
Jonathan David Groth

The cerebellum plays a crucial role in motor coordination along with basal ganglia and the motor areas of the cerebral cortex. Both somatosensory and the cerebro-cerebral pathways bring in massive amounts of neural information to the cerebellum. The output of the cerebellar cortex projects to various motor cortices as well as down to the spinal cord to make its contributions to the motor function.

The origin and function of the field potential oscillations in the cerebellum, especially in the high frequencies, have not been explored sufficiently. The primary objective of this study was to investigate the spatio-temporal characteristics of high frequency field potentials (150-350Hz) in the cerebellar cortex in a behavioral context. To this end, the paramedian lobule in rats was recorded using micro electro-corticogram (μ-ECoG) electrode arrays while the animal performed a lever press task using the forelimb. The phase synchrony analysis shows that the high frequency oscillations recorded at multiple points across the paramedian cortex episodically synchronize immediately before and desynchronize during the lever press. The electrode contacts were grouped according to their temporal course of phase synchrony around the time of lever press. Contact groups presented patches with slightly stronger synchrony values in the medio-lateral direction, and did not appear to form parasagittal zones. Spatiotemporal synchrony of high frequency field potentials has not been reported at such large-scales previously in the cerebellar cortex.

HIGH FREQUENCY FIELD POTENTIALS OF THE CEREBELLAR CORTEX

by
Jonathan David Groth

A Dissertation
Submitted to the Faculty of
New Jersey Institute of Technology
and Rutgers University-Newark
in Partial Fulfillment of the Requirements for the Degree of
Doctor of Philosophy in Biomedical Engineering

Joint Program in Biomedical Engineering

May 2015

.

APPROVAL PAGE

HIGH FREQUENCY FIELD POTENTIALS OF THE CEREBELLAR CORTEX

Jonathan David Groth

Dr. Mesut Sahin, Dissertation Advisor — Date
Associate Professor Biomedical Engineering, NJIT

Dr. Kevin Pang, Committee Member — Date
Professor of Neuroscience, Rutgers-Newark

Dr. Antje Ihlefeld, Committee Member — Date
Assistant Professor Biomedical Engineering, NJIT

Dr. Sergei Adamovich, Committee Member — Date
Associate Professor of Biomedical Engineering, NJIT

Dr. Viji Santakumar, Committee Member — Date
Associate Professor Neuroscience, Rutgers-Newark

BIOGRAPHICAL SKETCH

Author: Eyal Katz

Degree: Doctor of Philosophy

Date: August 2014

Undergraduate and Graduate Education:

- Doctor of Philosophy in Electrical Engineering,
  New Jersey Institute of Technology, Newark, NJ, 2014

- Master of Business Administration (MBA),
  Tel Aviv University, Tel Aviv, Israel, 1992

- Master of Science in Electrical Engineering (Magna Cum Laude),
  Tel Aviv University, Tel Aviv, Israel, 1989

- Bachelor of Science in Electrical Engineering,
  Tel Aviv University, Tel Aviv, Israel, 1984

Major: Electrical Engineering

Presentations and Publications:

E. Katz and Y. Bar-Ness, "Comparison of SNR and Peak-SNR (PSNR) Performance Measures and Signals for Peak-limited Two-Dimensional (2D) Pixelated Optical Wireless Communication", Accepted to Asilomar, November 2-5th, 2014, Pacific Grove, CA, USA.

E. Katz and Y. Bar-Ness, "Two-Dimensional (2D) Spatial Modulation Methods for Unipolar Pixelated Optical Wireless Communication Systems", Submitted for Publication.

E. Katz and Y. Bar-Ness, "Improved Channel Model for Two-Dimensional Pixelated Optical Wireless Communication Systems", to be submitted.

I dedicate this Dissertation to my family especially my parents. Without their support, I would not be where I am today. They raised me with love and wonder for the world around me. They taught me to always be curious and to have a respect for the scientific method in examining the way the world works. Over the years they have lent their ear to my troubles, given financial and moral support when I needed it, and directed me on my path both professionally and personally. Without them and the rest of my family, this Dissertation and who I am today would not have been possible.

ACKNOWLEDGMENT

I would like to thank Dr. Mesut Sahin for all the help and guidance that he has given over the years. I would like to thank the members of my committee, Dr. Sergei Adamovich, Dr. Keven Pang, Dr. Viji Santakumar, and Dr. Antje Ihlefeld for their input and direction for this dissertation.

I would like to thank Dr. Yi Guo for his design and implementation of the haptic lever set up and code without which this project would not have been possible.

I would also like to thank Dr. Abishek Prasad, Dr. Kohitj Kar, Dr. Gokhan Ordek, Dr. Soha Saleh, Dr. Yelda Alkan, and all those who I have met and worked with during my PhD for their input, help, and comradery.

TABLE OF CONTENTS

TABLE OF CONTENTS
(Continued)

Chapter **Page**

LIST OF FIGURES

LIST OF FIGURES

CHAPTER 1

INTRODUCTION

1.1 Objective

The cerebellum plays a crucial role in motor coordination along with the basal ganglia and the motor areas of the cerebral cortex (Houk and Wise 1995, Taniwaki, Okayama et al. 2006). Both somatosensory and the cerebro-cerebral pathways bring in massive amounts of neural information to the cerebellum primarily through pontine nuclei and the inferior olive to be processed (Ramnani 2006). The output of the cerebellar cortex projects to the deep cerebellar nuclei which send out axons back to various motor cortices as well as down to the spinal cord to make its contributions to the motor function (Ramnani 2006).

The cerebellar anatomy and neurophysiology has been extensively studied ever since the invention of early staining techniques and recording electronics. The relatively few type of cells involved in the cerebellar network and the crystalline network structure that is repeated across the cerebellar cortex have intrigued the neuroscientist for a long time and the cerebellum is often used as a model to study learning, plasticity, long-term depression, potentiation, etc. Despite its well-studied neurophysiology, the cerebellar function is still debated as to how it makes its contributions to motor coordination, the lack of which is evident in well-known clinical symptoms. An injury to the cerebellum does not cause paralysis, but a lack of synergy (ataxia) between the limb segments occurs (Javalkar, Kelley et al. 2014).

At the core of the problem lies the fact that the cerebellar circuitry has almost

always been studied at the cellular level in anesthetized animals. Very few reports are present in the literature that collected data in unanaesthetized animals using multi-contact electrode arrays. First, anesthesia completely suppresses the network activity of the cerebellar cortex, unlike the motor areas of the cerebrum (Hirono and Obata 2006, Bengtsson and Jörntell 2007, Ordek, Groth et al. 2013). Second, because the cerebellum is a center of motor coordination, it is impossible to understand its function with single electrode recordings without looking at the big picture. Many groups reported single and multiple electrode recordings in awake animals (Thach 1968, Bell and Grimm 1969, Lang, Sugihara et al. 1999, Heck, Thach et al. 2007, Ebner, Hewitt et al. 2011, Hewitt, Popa et al. 2011) and many studies applied calcium imaging techniques in the anesthetized animals (Tank, Sugimori et al. 1988, Sugimori and Llinás 1990, Stosiek, Garaschuk et al. 2003, Sullivan, Nimmerjahn et al. 2005, Díez-García, Akemann et al. 2007). However, what is needed to elevate the understanding of cerebellar function is to record with multi-electrode arrays from large areas of the cerebellar cortex to capture its network behavior in awake and behaving animals. Therefore, the proposal is to use an (ECoG) electrode to enable the recording of a large area of the cerebellum.

One of the defining features of the brain is the synchronous oscillations throughout the neocortex and with the substructures beneath (Buzsáki and Draguhn 2004, Buzsaki 2006). These synchronous oscillations are thought to solve the binding problem between different areas of the cortex thus allowing for faster processing and providing for a complete and unified perception of the environment (Buzsáki and Draguhn 2004, Buzsaki 2006). If this is true then the cerebellum should be bound in a similar way to allow for appropriate coupling and information sharing with the other areas of the brain.

It has been shown that granule layer of the cerebellum is coherent with the oscillations of the neocortex (O'Connor, Berg et al. 2002, Courtemanche and Lamarre 2005) and that these oscillation are able to entrain the granule layer and inferior olive neurons(Roš, Sachdev et al. 2009). However, it has not been demonstrated that Purkinje cells are entrained by the neocortical oscillations.

The hypothesis of this study is that the high frequency oscillations are related to movement and are modulated by neocortical oscillations. In order to show this the Very High Frequency Oscillations (VHFOs) will be looked at, between 150-350Hz, which have been shown to arise from the simple spike synchrony. If this is true, several things have to be seen. First, the VHFOs be related to the processing of the cerebellum and have a meaningful measure. Second, the VHFOs be related to the lower frequency oscillations which have been attributed to the granule and inferior olive circuits. Along these lines it has been demonstrated that the granule layer shows a very large scale synchrony of the theta oscillations, therefore, the VHFOs should show a similar large scale synchrony and this synchrony should also be functionally significant. Third, it should be demonstrated that the neocortical oscillations coherent with the cerebellum have similar frequencies and dynamics, also that the neocortex be shown to modulate the cerebellar VHFOs. To this extent we propose three aims.

Aim 1: Flexible micro-electrode arrays (MEAs) will be implanted for chronic recordings of spontaneously generated neural signals in behaving animals on the paramedian lobule of the cerebellar cortex as well as the forelimb area of the contralateral motor cortex. The 3D forces and torques generated by the forearm will be measured and the video images will be captured simultaneously during a lever pressing behavior. The damping and

spring coefficients of the lever arm will be controlled by the computer to simulate a viscous environment or a force field. VHFO synchrony within the cerebellum will be calculated and characterized during movement and rest. Using the strength of synchrony if it has a net directionality such as medio-lateral or rostro-caudal or if it is more of a uniform patchy distribution will be determined. This will inform which afferent fiber group that the synchrony may arise from.

Aim 2: For this aim, the same methods used in aim 1 will be used, however, we will now compare the synchronies in the VHFO range and theta band. The spatial organization of the synchrony in the VHFO range will also be analyzed. For this, the correlation techniques will be used to determine if the theta oscillations influence the VHFO synchrony.

Aim 3: ECoG electrodes will be placed on the primary motor cortex and the cerebellum. The theta band oscillations in both cortices will be compared using coherence and phase synchrony between the two regions. Stimulation of the motor cortex will be performed with varying frequency inputs. This will determine if the neocortical inputs can modulate the cerebellar VHFO synchrony and at which frequency the maximum modulation is achieved.

1.2 Background Information

The cerebellar cortex has a well-defined, highly organized structure (Figure 1.1). The same neural network pattern is repeated over and over in small units (microzones) (Apps and Garwicz 2005, Apps and Hawkes 2009). Most interestingly, this structural organization is preserved across the phylogenetic scale from fish to mammals (Sultan and

Glickstein 2007). Imaging studies in primates strongly supports the idea that cerebellum is not only involved in execution (Lotze, Montoya et al. 1999) of motor function but also in the planning phase (Hulsmann, Erb et al. 2003). When subjects were asked to perform a self-timed motor task, an early lateral cerebellar recruitment 2s prior movement onset was observed in fMRI images, confirming involvement of the cerebellum in the planning phase (Hulsmann, Erb et al. 2003). Another fMRI study showed that the cerebellum was also activated during imagined tool-use, and the centers of activity were located more laterally in the cerebellum than that evoked by the actual use of the tools (Higuchi, Imamizu et al. 2007). The side lobes areas are larger in the vertebrates that are higher in the phylogenetic scale (Sultan and Glickstein 2007). It is clear that the incoming information is processed in these lobes and sent back to various brain centers as well as the spinal cord through the cerebellar peduncles.

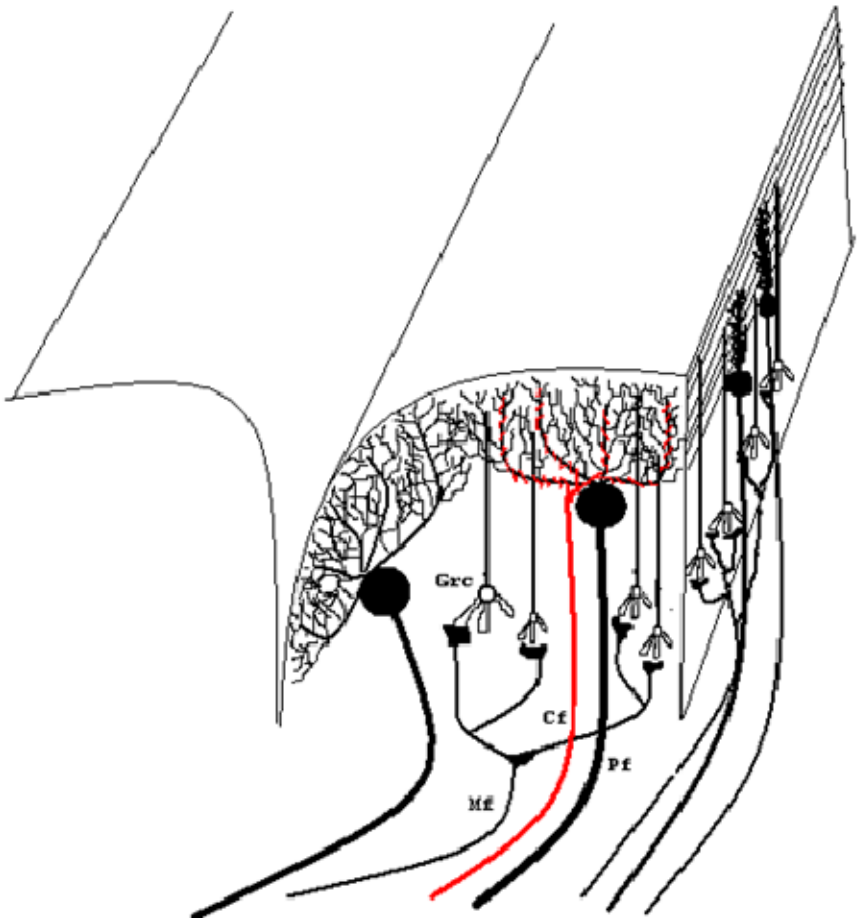

Figure 1.1 The cerebellar cortex with the Purkinje fibers (Pf), mossy fibers (Mf), granular cells (Grc), and climbing fibers (Cf).

The cerebellar cortex has three main layers: the granule layer, the Purkinje layer, and the molecular layer (Shepherd 2004). The granule layer has three main cell types. The granule cells which receive inputs and form the output of the granule layer (Shepherd 2004). The Golgi cells which are inhibitory interneurons of the granule layer (Shepherd 2004). The Lugaro cell which inhibits the Golgi cells (Shepherd 2004). The primary cell of the Purkinje layer is the Soma of the Purkinje cells which define this layer (Shepherd 2004). The molecular layer is mostly composed of the axon and dendrites from the granule, Golgi, and Purkinje cells (Shepherd 2004). The only cells that have their soma in the molecular layer are the Stellate cells which are inhibitory interneurons that synapse

onto the Purkinje cells at the base of their dendritic arbors (Shepherd 2004). The second is the basket cells, inhibitory neurons that synapse onto the Purkinje cell somas and receive their input from the molecular layer (Shepherd 2004).

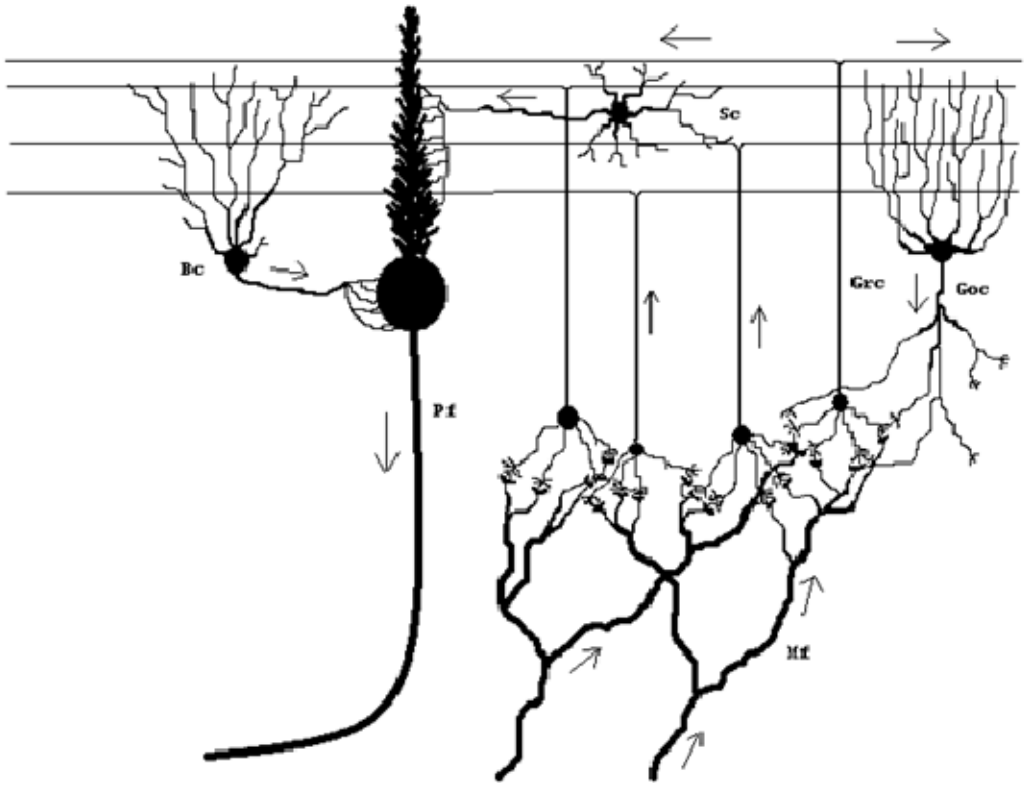

Figure 1.2 The mossy-granular-parallel fiber system, Purkinje cells (Pf), mossy fibers (Mf), granular cells (Grc), with inhibitory neurons, basket cells (Bc), stellate cells (Sc), and Golgi cells (Goc).

Both somatosensory and the cerebro-cerebellar pathways bring in massive amounts of neural information to the cerebellum, primarily through pontine nuclei and the inferior olive to be processed (Snider and Eldred 1951, Allen, Azzena et al. 1972, BRODAL 1978, Bower, Beermann et al. 1981, Andersson and Nyquist 1983, Tamada, Miyauchi et al. 1999, Salmi, Pallesen et al. 2009). These along with the inputs from the spino-cerebellar pathway form the major input called the mossy fibers (Anderson 1943,

Lundberg and Oscarsson 1960, Armstrong and Harvey 1968). The mossy fibers project into the granule layer, however, before that they form synapses in the deep cerebellar nuclei (Shepherd 2004). In the granule layer, the mossy fibers synapse onto the granule and Golgi cells forming synaptic bundles called glomeruli (Shepherd 2004).

The outermost layer of the cortex, the molecular layer, contains granule cell axons known as parallel fibers that run parallel to the long axis of the folia in the medio-lateral direction (Shepherd 2004). The Purkinje cells, found in the next layer below, send their dendrites up into the molecular layer where they branch extensively (Shepherd 2004). The parallel fibers bifurcate as they reach the surface and run several millimeters in the mediolateral direction on each side (Shepherd 2004). These fibers intersect the dendrites of several thousand Purkinje cells that are oriented perpendicular (in rostro-caudal direction) to the parallel fibers (Shepherd 2004). Each Purkinje cell receives converging inputs from up to 200,000 parallel fibers of granule cells. Considering there are about 107 Purkinje cells in the cerebellum, the total number of synaptic connections and hence the computational power is immense (Shepherd 2004). Purkinje cell axons provide the sole output of the cerebellar cortex to other brain centers (Shepherd 2004).

The layer below the Purkinje cell layer is the granule cell layer. The primary excitatory cell in this layer is the granule cell whose axons form synapse on to the Purkinje cells in two ways. The parallel fibers synapse onto the Purkinje cells at the level of the dendrites (Huang, Wang et al. 2006). The granular cells axons also synapse onto the Purkinje cell along the ascending axon (Huang, Wang et al. 2006). The primary inhibitory cells in the granule layer are the Golgi cells which inhibit the granular cells (Shepherd 2004). The input to the granule cells is the mossy fiber system that constitutes

the largest contingent of cerebellar afferents. They originate from a variety of brain stem nuclei that receive input from the cerebral cortex and the spinal cord (Shepherd 2004). A major flow of information exists from the cerebral cortex to the cerebellum (Snider and Eldred 1951, Allen, Azzena et al. 1972, Brodal 1978, Bower, Beermann et al. 1981, Andersson and Nyquist 1983, Tamada, Miyauchi et al. 1999, Salmi, Pallesen et al. 2009). The cerebro-cerebellum, which makes up the large lobes on each side of the cerebellum, receives information from wide areas of the cerebral cortex (Snider and Eldred 1951, Allen, Azzena et al. 1972, Brodal 1978, Bower, Beermann et al. 1981, Andersson and Nyquist 1983, Tamada, Miyauchi et al. 1999, Salmi, Pallesen et al. 2009). Axons arising from pyramidal cells in the sensorimotor cortex-frontal areas 4 and 6, somatosensory areas on the postcentral gyrus, and the posterior parietal areas- form a massive projection to the clusters of cells in the pontine nuclei, which in turn feed the cerebellum (Mizuno, Mochizuki et al. 1973). The second afferent input to the cerebellum is the climbing fiber system (red axons in Figure 1.1) that originate in the inferior olive (Andersson and Nyquist 1983). Both mossy and climbing fiber systems carry information from the central inputs as well as the periphery to the cerebellum (Shepherd 2004).

The granule cells are glutamatergic cells that project up to Purkinje cells (Shepherd 2004). There are two types of synapses that the granule cells form. The first is the parallel fiber pathway. In this pathway, the granule cells project up to the molecular layer where they then bisect into two oppositely projecting axons that run parallel to the other granular cell projections (Shepherd 2004). These axon projections run in the coronal direction while the Purkinje cells form a plane in the parasagittal direction thus the granular cell axons run in an orthogonal direction to the Purkinje cell

arbors (Voogd and Glickstein 1998). The parallel fibers, as they are called, extend out several millimeters thus passing through several Purkinje cells (Shepherd 2004). The second synapse formed by the granule cells is formed on the soma of the Purkinje cells by the rising axon (Huang, Wang et al. 2006). This axon is believed to from a much stronger synapse than those formed on the dendrites by the parallel fibers (Huang, Wang et al. 2006).

The second major cell of the granule layer is the Golgi cell. The Golgi cells form GABAergic synapses onto the granule cells (Shepherd 2004). The Golgi cells sit primarily in upper region of the granule layer, just below the Purkinje cells, however, they can be found through all parts of the granule layer (Shepherd 2004). The Golgi cells send off two sets of dendrites, the first remains in the granule layer forming part of the glomeruli (Shepherd 2004). The second rise up the molecular layer (Shepherd 2004). The Golgi cells receive synapses from two sets of neurons. The first is from the mossy fibers in the glomeruli. The second is from the parallel fiber in the molecular layer (Shepherd 2004). The Golgi cells synapse onto the granule cells providing an inhibitory input (Shepherd 2004). These two inputs to the Golgi cells form a feed forward and feedback inhibition to the granule cells.

The mossy fiber system gives rise to what is called 'fractured somatotopic organization' in the cerebellar cortex (Shambes, Beermann et al. 1978, Shambes, Gibson et al. 1978). This is dramatically seen in the detailed maps obtained in the rat (Shambes, Gibson et al. 1978). Each peripheral location projects to a sharply demarcated area, which is in contrast to the cerebral cortex where the somatotopic maps are 'fuzzy' and overlapping (Shambes, Gibson et al. 1978). On the other hand, the climbing fiber system

forms parasagitaly oriented functional units that are called ‘microzones’ (Andersson and Oscarsson 1978). Both of these somatatopic organizations are major advantages for signal processing and interpretation of the neural data in this project.

The granule cell layer is believed to perform a spatio-temporal filtering on the inputs from the mossy fibers (D'Angelo 2008, D'Angelo, Solinas et al. 2013). Oscillations in the 4-25Hz range originate primarily from the granule layer (Pellerin and Lamarre 1997, Hartmann and Bower 1998). The granule cells also show a resonance in the 4-10Hz range (D'Angelo, Nieus et al. 2001). The Golgi cells show a resonance and pace making in the same range however, it has been shown the granule cell resonance may be independent of the Golgi cell pacemaking (Solinas, Forti et al. 2007, Solinas, Forti et al. 2007, D'Angelo, Solinas et al. 2013). This resonance results in a large scale synchrony in the theta range across the granule layer (Courtemanche and Lamarre 2005).

Purkinje cells are the largest and only output in the cerebellar cortex (Shepherd 2004). The Purkinje cells have a spontaneous activity of 30-40Hz spike rate. With incoming input from the granule cells Purkinje cells fire at a rate of 50-100Hz (D'Angelo, Koekkoek et al. 2009). Purkinje cells have been shown to have a high synchrony between simple spikes. The simple spike synchrony is believed to arise from parallel fibers, climbing fibers, or Purkinje cell axon collaterals. Synchrony is believed to act on the deep cerebellar nuclei in one of two ways. The first is that Purkinje cells, being inhibitory, inhibit the deep cerebellar nuclear cells. The second way, which has been recently demonstrated, that there can be an after inhibition rebound spiking in the deep cerebellar nuclear cells.

First discovered in the 1930s, the Purkinje layer shows an oscillation rate from 150-350Hz (Adrian 1934). These oscillations are at a much higher frequency than the firing rate of the individual neurons. It has been shown that these oscillations are generated in the Purkinje layer. It has been shown that, while Purkinje cells do not fire at such a high frequency, they do synchronize in the population of Purkinje cells at this rate. Therefore, these VHFOs mostly represent the Purkinje cell synchronization.

Cerebellar field potentials have been demonstrated to be coherent with the neocortical LFPs bellow 30Hz (Courtemanche and Lamarre 2005). This coherence is mostly due to granular LFPs (Courtemanche and Lamarre 2005). The cerebellum seems to have little to no effect on the oscillations of the neocortex (Popa, Spolidoro et al. 2013). It has also been shown that the neocortical oscillations entrain the granule cells and Golgi cells such that there is an increased firing rate during the up states of the oscillations (Roš, Sachdev et al. 2009). The inferior olive has also been demonstrated to show an entrainment with the neocortical oscillations (Roš, Sachdev et al. 2009). Given the entrainment of the granule layer and the inferior olive with the neocortical oscillations it would be expected that the Purkinje cells also show an entrainment however, the Purkinje cells entrainment was very week though these experiments were performed under anesthesia which has been shown to disrupt cerebellar circuitry (Roš, Sachdev et al. 2009). This presents a problem on how are the neocortical oscillations that so prevalently affect the other areas of the cerebellar circuit are carried to the deep cerebellar nuclei.

The 4-25 Hz oscillation range is one of the most studied oscillations in the cerebellar cortex. The oscillation was originally discovered in primates and rodents

(Pellerin and Lamarre 1997, Hartmann and Bower 1998). The oscillations are at two different frequencies; 14-20Hz in primates and 7-8Hz in rodents (Pellerin and Lamarre 1997, Hartmann and Bower 1998). Though they are at different frequencies they contain many similarities. They both arise out of the granular layer (Pellerin and Lamarre 1997, Hartmann and Bower 1998). They both are at maximum amplitude during similar activity states (Pellerin and Lamarre 1997, Hartmann and Bower 1998). Both show a spindle shaped wave form (Pellerin and Lamarre 1997, Hartmann and Bower 1998). These oscillations are now widely recognized to be the same oscillations with the same function it both groups.

These oscillations, are best recorded from the granular layer. They show a strong similarity to the granular layer multi-unit activity (Courtemanche, Pellerin et al. 2002, Lu, Hartmann et al. 2005). They also demonstrate a similarity to the Purkinje cell activity however, this is weaker than the granular layer activity (Courtemanche, Pellerin et al. 2002, Lu, Hartmann et al. 2005). No similarity was demonstrated to the climbing fiber activity (Courtemanche, Pellerin et al. 2002). From this it can be seen that the most obvious origin for the oscillations are the granular layer cells.

Early experiments showed that the largest amplitudes are seen when the animals are at rest (Pellerin and Lamarre 1997, Hartmann and Bower 1998). These oscillations would occurred during the time that the animal was attentive and immobile (Pellerin and Lamarre 1997, Hartmann and Bower 1998). As soon as the animal began its movement, the oscillations ceased (Pellerin and Lamarre 1997, Hartmann and Bower 1998). These oscillations showed a spindle shaped waveform lasting for several seconds which waxed and waned in the period (Pellerin and Lamarre 1997, Hartmann and Bower 1998).

These oscillations were also shown to have a strong relationship with the multi-unit activity of the granular layer (Courtemanche, Pellerin et al. 2002). The multi-unit activity had a decreased spike rate during the oscillations (Courtemanche, Pellerin et al. 2002). When the oscillations stopped, there was a 2-3 times increase in the spike rate (Courtemanche, Pellerin et al. 2002). The Purkinje cell simple spike rate also showed a relationship to the oscillations (Courtemanche, Pellerin et al. 2002, Lu, Hartmann et al. 2005). Similarly to the granular layer multi-unit activity, the simple spike activity showed an increase with the cessation of the oscillatory activity (Courtemanche, Pellerin et al. 2002). Interestingly, the granular multi-unit activity showed near zero delays to the oscillatory activity in the cross-correlation however, the Purkinje cell simple spike precede the cessation by a period of ~10ms (Courtemanche, Pellerin et al. 2002).

Later, experiments showed that the oscillations were not due to movement preparation alone (Hartmann and Bower 1998, Courtemanche, Pellerin et al. 2002). They showed that the oscillations increased after stimulus, which indicates a waiting period before a movement occurs, then a decrease when the movement is initiated (Courtemanche, Pellerin et al. 2002). The oscillations tend to last the entire time of the waiting period (Courtemanche, Pellerin et al. 2002). This shows that the oscillations are related to the expectation of a motor output. However, they were also active when the animals were expecting a reward but not about to move (Courtemanche, Pellerin et al. 2002). This showed that the oscillations increased after a stimulus, indicating a waiting period for a reward, after the award was given the oscillations showed a sharp decrease (Courtemanche, Pellerin et al. 2002). These shows that the oscillations represent a state of a more abstract anticipation of some event.

These oscillations have also been shown to be related to the cortical oscillations in the same frequency range. The oscillations in the primate paramedian lobule and cerebral cortex showed a similar modulation of the 10-25Hz oscillation (Courtemanche and Lamarre 2005). They also showed a significant synchronization with a peak correlation around zero lag (Courtemanche and Lamarre 2005). The highest synchronization was seen in the primary sensory cortex (S1) however, the primary motor cortex (M1) also showed some synchronization (Courtemanche and Lamarre 2005). There was synchronization for both the passive expectancy, where there was no movement but an expectation of reward, and the lever press task (Courtemanche and Lamarre 2005). The lever press task showed a significantly high correlation to the S1 oscillations than did the passive expectancy (Courtemanche and Lamarre 2005). These oscillations, however, do not appear to be caused solely by the cortical oscillations. The correlation coefficients in some states such as rest with no expectancy showed much lower correlation coefficients than that in passive expectancy or before a motor task (Courtemanche and Lamarre 2005).

This relationship brings up a question, does the cerebellum just pass the oscillations from the cortex or does it play a role in creating and perpetuating these oscillations. Looking at the cellular profiles of the cerebellar granule layer shows that the cells do have resonant properties that are responsible for enhancing these oscillations. Granule cells have been shown to be resonant in the theta frequency and experience bursting capabilities (D'Angelo, Nieus et al. 2001). The Golgi cells also show a resonance in the theta band (Solinas, Forti et al. 2007, Solinas, Forti et al. 2007). They also show a pace making and bursting capabilities in the theta band (Solinas, Forti et al.

2007, Solinas, Forti et al. 2007, D'Angelo 2008). The mossy fiber synapses show long term potentiation (LTP) at the granule cell synapse which may be responsible for improved spike timing (D'Angelo 2008, D'Angelo and De Zeeuw 2009). All of these combine to create an oscillating circuit that produce tight timed windows for signals coming from the mossy fibers.

There are two somatotopic maps in the spinocerebellar region one on the anterior and one on the posterior faces (Adrian 1943, Shambes, Gibson et al. 1978, Bower, Beermann et al. 1981). However, the somatotopic maps are not composed of continuous areas representing a certain region of the body rather they are composed of a mosaic of patches called fractured somatotopy (Shambes, Gibson et al. 1978). This means that the regions for a particular body region are represented on the cerebellar cortex by several small patches for particular parts of a region broken up by patches for other regions for example the forearm and paw are broken up by regions of the face and jaw on the paramedian lobule (Shambes, Gibson et al. 1978). The climbing fibers form the basic organization for these regions (Armstrong, Harvey et al. 1971). The mossy fibers and climbing fibers for the same region of the body rise to the same areas in the cerebellar cortex (Odeh, Ackerley et al. 2005). However, the mossy fibers form slightly larger patches than do the climbing fibers (Odeh, Ackerley et al. 2005).

Several models have been proposed on how the cerebellum processes the information and how the brain uses its output. Kawato and Gomi proposed a feedback-error-learning scheme were the climbing fibers represent an error signal (Kawato and Gomi 1992). Kettner et al proposed a predictive control model for the cerebellar control of smooth eye pursuits (Kettner, Mahamud et al. 1997). Hirano proposed the cerebellum

is involved in feed-forward associative learning (Hirano 2006). Recently, these two models have been combined with the idea of the cerebellum as a place for internal model creation. There are two forms of internal models that are being looked into, the inverse model (Kawato 1993, Shidara, Kawano et al. 1993, Schweighofer 1998, Nowak, Topka et al. 2007) and the forward model (Nowak, Topka et al. 2007, Shadmehr and Krakauer 2008). The inverse model would use sensory information about the limbs kinematics and develop the appropriate motor signal to compare versus the actual motor signal (Manto and Bastian 2007). The forward model use efferent copies of motor commands and predict sensory consequences (Manto and Bastian 2007).

The field potentials for the mossy fiber volleys were first detailed by Eccles et al in 1967 (Eccles, Sasaki et al. 1967). They studied the mossy fiber volleys by juxta-fastigial stimulation, stimulation of the deep white matter of the cerebellum, and trans-folial stimulation, stimulation of an adjacent folium's molecular layer. They recorded the field potential using a micro electrode at varying depths in the cerebellar cortex. This allowed them to determine the region and thus the structures that gave rise to the individual components.

To understand where the field potentials may arise, it is useful to look at the evoked potentials. While these represent an overly synchronized epoch of activity they are still valuable in understanding which cell sources may be picked up from the surface. Eccles was the first to map the evoked potentials to their respective cellular sources.

The results showed that the components of the field potentials arise from distinct regions of the cortex. The P1/N1 wave had the normal form of an impulse traveling up a nerve and thus arises from the propagation of the action potentials up the mossy fiber

axons. The N2 was strongest in the granular layer and had the form of a slow excitatory post synaptic potential (EPSP). They determined that it was due to the excitation of the granule and Golgi cells. The P2/N3 wave arose simultaneously from the transmission of the impulse up the granular cells and the excitation of the Purkinje cells. The P2 wave was detected while recording in the granular layer and lower and the N3 wave was detected in the molecular layer. The N4 wave was the result of the impulse traveling down the Purkinje axon. The P3 wave was believed to be produced by the IPSP of the inhibitory neurons in the cerebellar cortex (Eccles, Sasaki et al. 1967). Figure 1.6 shows a graphical representation of the origin of the mossy fiber field potential and Figure 1.7 shows the results of Eccles experiments showing the mossy fiber potentials at varying depths.

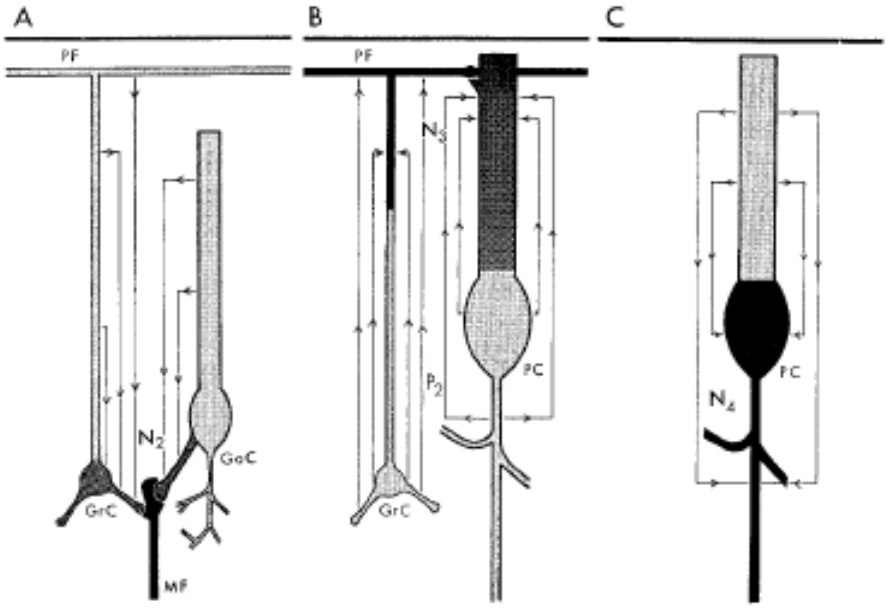

Figure 1.3 Graphical representation of the origin of the potential fields. The N1 wave, not shown, arises from the impulse traveling along the mossy fiber. The N2 wave arises from the EPSP on the granular cells and Golgi cells. The P2/N3 wave arises from the Impulses traveling up the granular cell axon and the EPSP of the Parallel fibers on the Purkinje cells. The N4 wave arises from the impulse traveling down the Purkinje fiber.
Source: [Eccles, J. C., Sasaki, K., Strata, P., "Interpretation of the potential fields generated in the cerebellar cortex by a mossy fiber volley," Experimental Brain Research, vol. 3, pp. 58-80, 1967]

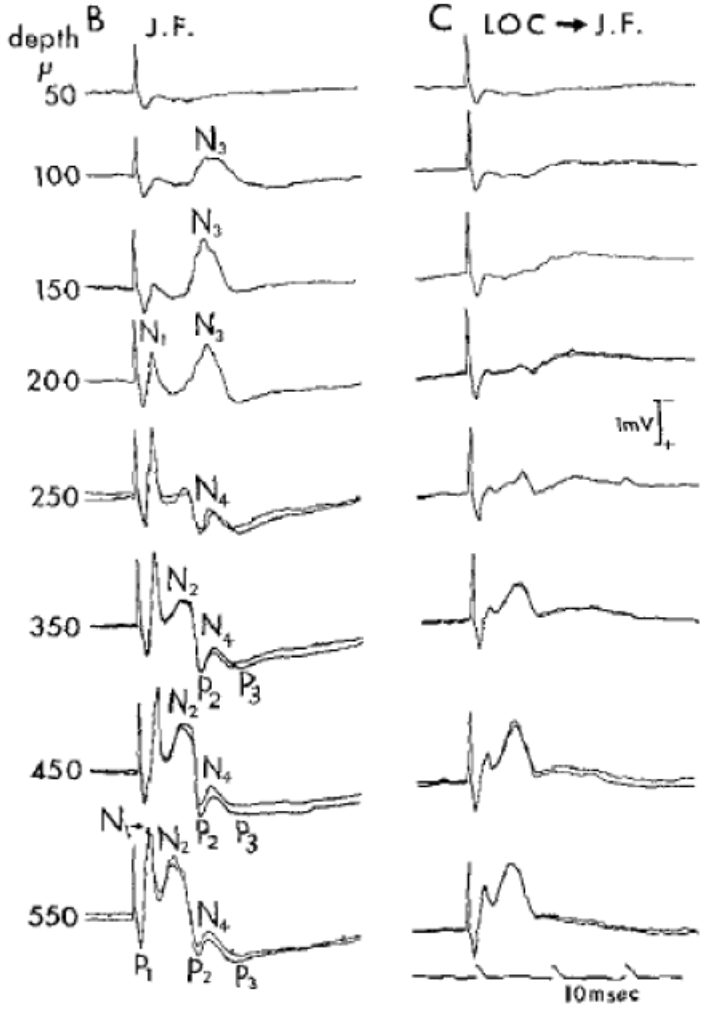

Figure 1.4 The results of Eccles et al experiments showing the mossy fiber field potential at varying depths. The P1, N1, N2, N2, P2, N4, and P3 waves are marked for each depth.
Source: [Eccles, J. C., Sasaki, K., Strata, P., "Interpretation of the potential fields generated in the cerebellar cortex by a mossy fiber volley," Experimental Brain Research, vol. 3, pp. 58-80, 1967]

Armstrong et al. (Armstrong and Drew 1980) performed a similar experiment though they stimulated the cutaneous afferent fibers and recorded on the pial surface.

They showed that the surface recordings were the similar to those recorded in the molecular layer. They also showed that the N1 peak occurred at a latency of approximately 2.4ms. The N1 peak was followed by the N2 peak and N3 peak. The N3 peak occurred at a latency of 5.0ms. The results of their experiments are shown in Figure 1.8.

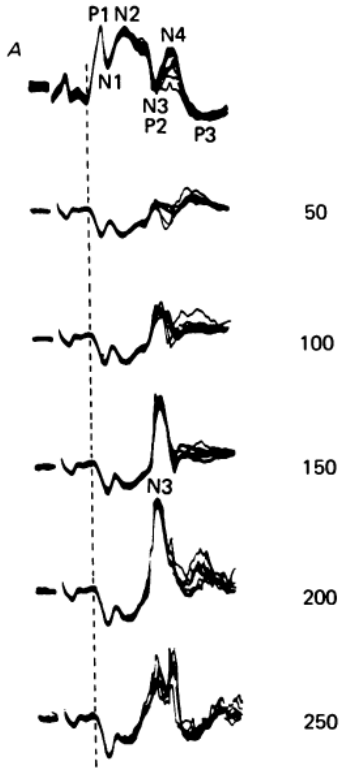

Figure 1.5 The results of the Armstrong et al. experiments showing the mossy fiber field potentials, evoked by stimulation of the cutaneous afferents, at varying depths. The top plot represents the surface field potential and the components are marked.
Source: [Armstrong, D. M., Drew, T., "Responses in the posterior lobe of the rat cerebellum to electrical stimulation of cutaneous afferents to the snout," Journal of Physiology, vol. 309, pp. 357-374, 1980.]

These results demonstrate that the field potentials for the cerebellar cortex arise from all layers of the cortex. Armstrong's work which used a ball electrode on the surface of the cerebellum showed that all the wave forms are present. The N2 wave and the N4 wave show that the granule layer and Purkinje layer potentials from the surface

represent similar amplitude. So it would be expected that the source of the field potentials in the cortex recorded from the surface will contain both the components of the granule layer and the Purkinje layer in an equal fashion. This is not surprising due to the cellular structure of the cerebellum. The granule cells are small but densely packed with many cells receiving common input from the mossy fiber axons. This will cause a dense synchronous depolarization within the granular cells causing a large field potential. The Purkinje cells are a very large cells with a large dendritic arbor receiving many connections from the granule layer. The third major source of the field potentials is the climbing fiber with produce very robust depolarizations in the Purkinje cells. These a single climbing fibers will synapse exclusively on several Purkinje cells. The inferior olive, where the climbing fibers originate, also have a large about of gap junctions between them. This combines to from a very robust depolarization across a number of Purkinje cells which produces a large field potential.

CHAPTER 2

RESULTS

2.1 Very High Frequency Modulation with Movement

The cerebellum is essential to sensory-motor integration for fine control of motor performance. It has also been shown to be important in many cognitive tasks of the brain (Schmahmann 2010). There are two main afferent pathways to the cerebellum. The first is the mossy fiber pathway which originates from a number of cerebral areas and the spinal cord and terminates in the granular layer of the cerebellar cortex where they synapse onto the granule cells, which then synapse onto the Purkinje cells (Eccles, Sasaki et al. 1967, Ito 2010). The second is the climbing fiber pathway that originates in the inferior olive and projects directly onto the Purkinje cells (Voogd, J., et al. 1981, Voogd, J. and M. Glickstein 1998, Buisseret-Delmas, C. and P. Angaut 1993, Apps, R. and M. Garwicz 2005, Sugihara, I., et al. 1999). The different input pathways and their termination on the Purkinje cells form the basic processing unit in the neural circuitry of the cerebellar cortex. The sensory mossy fiber inputs to the granular cells form a patchy architecture (Shambes, Gibson et al. 1978) while the climbing fiber inputs form microzones oriented in the parasagittal direction (Garwicz, Ekerot et al. 1998, Garwicz, Jorntell et al. 1998). These two architectures are believed to be functionally overlapping in what is called the one map theory (Apps and Hawkes 2009, Cerminara, Aoki et al. 2013). Current understanding of the cerebellar function is mostly built upon the cerebellar anatomy and single cell recording data collected using indwelling electrodes. Cellular level neural signals are important to understand how the cerebellar circuity

processes information. On the other hand, multi-channel field potential recordings in behaving animals can provide direct evidence on the cerebellar function at a larger scale.

The cerebellum is known to express several types of oscillations arising from different cortical layers. Oscillatory activity is an important part of neural function and is present throughout the brain. Oscillations have been reported to help shape the timing and binding of the actions of neurons into a cohesive representation in both local circuits and across regions in the brain (Buzsáki and Draguhn 2004, Buzsaki 2006). These rhythms are necessary to create a unified picture of the world and motor responses (Buzsaki 2006).

Two oscillations that have recently garnered interest in the cerebellum are the very slow (~1Hz, see (Ros, Sachdev et al. 2009)) and the 4-25Hz oscillations that originate in the granule cell layer (Pellerin and Lamarre 1997, Hartmann and Bower 1998, D'Angelo, Nieus et al. 2001, Courtemanche, Pellerin et al. 2002). The granule cells also show a resonance in the 4-10Hz range (D'Angelo, Nieus et al. 2001). The Golgi cells of the molecular layer show a resonance and pace making in the same range, however, it has been argued that the granule cell resonance may be independent of the Golgi cell pacemaking (Solinas, Forti et al. 2007, Solinas, Forti et al. 2007), (D'Angelo, Solinas et al. 2013). The 4-25Hz oscillations show a strong similarity to the granular layer multi-unit activity, a weaker one to the Purkinje cell activity ((Courtemanche, Pellerin et al. 2002), (Lu, Hartmann et al. 2005)), and no correlation to the climbing fiber activity (Courtemanche, Pellerin et al. 2002).

Another major oscillation type found in the cerebellum is the fast oscillations. The high frequency cerebellar oscillations in the 150-250Hz range were first discovered

by Adrian in 1934 (Adrian 1934). It was later shown that the fast frequency components are related to the state of the animal (Oehler, Pickenhain et al. 1969). They appeared during preparation for goal directed movements but not during non-goal directed repetitive movements. These high frequency field potentials have been shown to originate from the Purkinje cell layer and are believed to be the result of Purkinje cell simple spike synchrony (Cheron, Servais et al. 2004, Cheron, Servais et al. 2008, de Solages, Szapiro et al. 2008, Middleton, Racca et al. 2008). There are several theories as to how this spike synchrony arises. One theory is that the synchrony is caused by common inputs such as the mossy fibers (Heck, Thach et al. 2007). Another theory is that the synchrony is caused by the inhibitory Purkinje axon collaterals (de Solages, Szapiro et al. 2008). The most probable case is that it is a combination of multiple influences.

Purkinje cell synchrony may play an important role in cerebellar information processing. There is evidence that the cerebellum may encode information in the spatiotemporal domain (Isope, Dieudonné et al. 2002, De Zeeuw, Hoebeek et al. 2011). It has recently been shown that synchronous inhibition of the deep cerebellar nuclei (DCN) by the Purkinje cells can lead to rebound firing of the DCN cells, which can modulate the motor output (Witter, Canto et al. 2013). Therefore, synchronous spiking of Purkinje cells has been proposed to play an important role in cerebellar signal processing and thus the cerebellar function.

For these reasons, an investigation of high frequency field potentials in the cerebellar cortex could provide important clues to the function of and information processing in the cerebellum. However, these cerebellar oscillations have not been as

extensively studied as in other areas of the brain such as the hippocampus. In this study we investigated the spatio-temporal patterns of high frequency synchrony in the cerebellar cortex during goal directed movements in order to better understand their functional role. We employed chronically implanted μ-ECoG electrode arrays for the first time to capture the field potentials from the cerebellar surface without penetrating the cortex. The use of a μ-ECoG array allowed us to study synchrony between 31 different sites covering relatively a large area of the PML cortex in the same preparation. Chronic implantation of the array also made it possible to record these signals in behaving animals in multi-day trials for a few weeks.

2.1.1 Methods

The animals were trained for the lever pressing task prior to implant surgery. The lever was attached to a robot with haptic feedback (Falcon, Novint Inc., Albuquerque, NM) that simulated a viscous environment with programmable parameters via the computer. A food reward (sugar pellet) was delivered through a tube located a few centimeters to the left of the lever once the lever was pressed. The animals were placed on food restriction a few days prior to training. During, training animals were allowed to freely roam the cage. The trial was initiated by a computer-generated beep sound. After the beep, the animals could press the lever any time within the following 5 second window. The 5 second data segment containing the lever press in the middle of the episode was saved by the computer for later analysis. The rats learned this behavior usually within a week by training about 30 minutes each day. The proximity of the lever to where the sugar pellet drops sometime allowed the rats to rest the arm on the lever while picking the

sugar pellet with their mouth. The trials that did not start with the hands on the floor were excluded from the analysis

Micro-ECoG arrays were chronically implanted in three Long Evans rats (350-450g) using sterile surgical techniques. All procedures were approved and performed in accordance to the guidelines of the Institutional Animal Care and Use Committee, Rutgers University, Newark, NJ. The rats were anesthetized with ketamine and xylazine (100mg/kg and 10mg/kg respectively, IP) and additional doses were administered as needed during the surgical procedure. The skull over the right paramedian lobule (PML) of the cerebellum was removed and a 'T' shape cut was made into the dura using fine scissors. A custom-design, flexible substrate (12 µm polyimide), 32-contact electrode array (NeuroNexus, MI) was placed subdurally by sliding it through the dural cut on the right paramedian cortex with the medial edge of the electrode positioned about 1 mm away from the paravermal vein and fixed in place with very small amounts of cyanoacrylate (gluture, WPI Inc.) at four corners to the cortical surface (Figure 2.1). Electrode contacts were 50 µm in diameter and located 300 µm apart from each other in a 4x8 configuration, hence covered approximately 900 x 2100 µm of the PML in the medio-lateral orientation as shown in Figure 2.1. The dura was sealed with a fast curing silicone elastomer (Kwik-Cast, WPI Inc.) over the array. A stainless steel wire that served as a reference electrode was laid down over the area on the backside of the array and secured in place with cyanoacrylate. The Omnetics micro connector at the end of the ribbon cable was fixed on the skull using dental acrylic and five stainless steel screws. The recordings started about a week after surgery with a 31-channel head-stage amplifier (Gain=100, TBSI, NC) inserted into the micro connector on the head while animals were

placed in a large Faraday cage. The signals were sampled at 20 kHz in 5 second episodes containing the behavior.

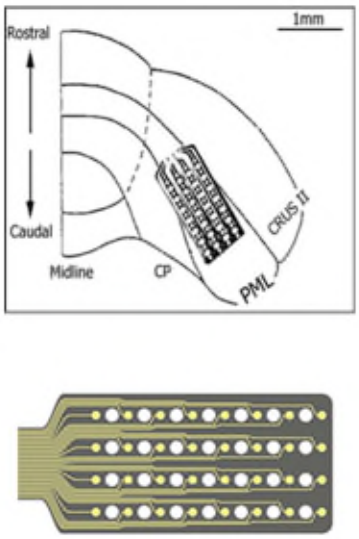

Figure 2.1. The implant location of the recording array is depicted on the right paramedian lobule (PML) of the posterior cerebellum. The 4x8 arrangement of the contacts on the micro-electrode array is also shown at a large scale on the bottom. A few contacts fell outside the paramedian lobule because of medially narrowing shape of the PML.

All data analysis was performed using Matlab (Mathworks, Natick, MA). The power spectrum was calculated using the multitaper method for each trial and channel using the Chronux toolbox (Bokil, Andrews et al. 2010). Power spectra were then averaged across all trials and channels. The spectrograms were also calculated using multitaper method with a window length of 200ms and a step size of 100ms. The inter-contact coherence spectra were computed and averaged between all channel combinations in each trial using Matlab's *mscohere* function (Hamming window, 50% overlap), which is a magnitude squared coherence estimate with values between 0 and 1 that indicate how well one signal corresponds to another at each frequency. The

coherence is a function of the power spectral densities, $P_{xx}(f)$ and $P_{yy}(f)$, of x and y, and the cross power spectral density, $P_{xy}(f)$, as given below:

$$C_{xy}(f) = \frac{|P_{xy}(f)|^2}{P_{xx}(f) * Pyy(f)} \tag{1.1}$$

In order to produce the coherogram plots, i.e. coherence as a function of time and frequency, the inter-contact coherence spectra were computed within a 200ms window (also Hamming windowed with 50% overlap) that was shifted in 100ms steps for the entire duration of the trial.

For phase synchrony we developed our own Matlab code based on the analysis method described in (Tass, Rosenblum et al. 1998). In brief, the phase information in each neural channel was found from the analytic signal of the Hilbert transformation as a function of time in a running window. The Hilbert transform and the phase signal are computed by the following equations respectively.

$$HT(x)(t) = \frac{1}{\pi} * CPV \int_{-\infty}^{\infty} \frac{x(\tau)}{t-\tau} d\tau \tag{1.2}$$

$$Ax(t) = x(t) + jHT(x)(t) \tag{1.3}$$

Where x(t) is the signal to be transformed and HT(x)(t) is the Hilbert transform of x(t). CPV represents the Cauchy principle value method of integration. The phase signal is represented by Ax(t). The differential phase between channels was computed for each channel pair in a running window over time. Shannon entropy was computed and used as a synchrony measure from the statistics of inter-channel synchrony given the assumption that two signals are synchronous for a given time window when their differential phase is approximately constant. The Shannon entropy index was given by:

$$\gamma = (Hmax - H)/Hmax \tag{1.4}$$

With the entropy (H) given by:

$$H = \sum_{k=1}^{N} pk * \ln(pk) \tag{1.5}$$

The value of N is the number of phase bins defined by N=exp[0.626 + 0.4 * ln(M−1)] where M is the number of time samples within the running window (200ms). The value p_k is the relative frequency of differential phases within the k^{th} bin. H_{max} is defined as H_{max}=ln(N). Synchrony values (γ) of 0 and 1 meant no synchrony and perfect synchrony, respectively.

In addition, clustering analysis was performed on the inter-contact synchrony values to determine which channels followed a similar trend as a group around the time of lever press and if there was a spatial pattern to the synchrony. The synchrony values were averaged across the frequency band of interest (150-350Hz) between all contact pairs during lever press in multiple trials. A long vector was formed for each contact that consisted of its synchrony values with all the other contacts as a function of time (11 time points at 50ms intervals) and in multiple trials. In other words, each vector contained many small vectors of 11 synchrony values, concatenated with other small vectors resulting from multiple trials and with multiple contacts. This way all the variation across the trials was contained in one large vector by combining the inter-contact synchrony data from all trials. The synchrony vectors from all 31 contacts were then clustered using the k-means method in Matlab. Since the clusters were observed to change between clustering attempts, one thousand clustering iterations were implemented

with randomized starting points. This accounted for the variations in clustering due to the dependency of the algorithm on the starting points. The success rates of clustering together were calculated between each contact pair. Contact pairs that ended up in the same cluster in greater than or equal to 95% of the attempt were considered to be in the same group. After the final groups were derived, the centroids of the contact groups (i.e. their vectors) and Euclidian distances from the centroid to each vector were calculated. The strength of membership for each contact to a group was calculated using the following equation.

$$SM = 1 - \frac{D1}{\frac{\sum Dn}{N}} \quad (1.6)$$

Where SM is the strength of membership for which 1.0 is the highest value and lower values represent weaker membership to a group. D1 is the Euclidian distance of a contact to the centroid of its own group. The numerator represents the average distance of a contact to the centroids of all the groups.

2.1.2 Results

μ-ECoG signals of the PML were analyzed during a lever pressing task. The high frequency components (150-350Hz) were present in all recordings and showed oscillatory patterns with rapidly changing amplitudes during the movements of the animal (Figure 2.2). However, a direct correspondence between the instantaneous signal amplitudes and the motor behavior was not observed. The multi-channel signals were seen to move in and out of synchrony in short episodes. Those episodes with high inter-contact synchrony tended to have larger amplitudes since synchronous field potentials

add constructively at the recording sites in a volume conductor. The neural signal power spectrum typically extended up to 900Hz (active plot in Figure 2.3) beginning to drop only after 300Hz, and a dip was observed with its center in the beta frequency range (inset). The power spectra of these 5 s long recording epochs did not have a sharp peak, which would indicate oscillations at a single or a narrow band of frequencies. There was a clear difference in signal power between the active and quiet states of the animals, defined as quietly sitting in the cage in awake state with no visible movements.

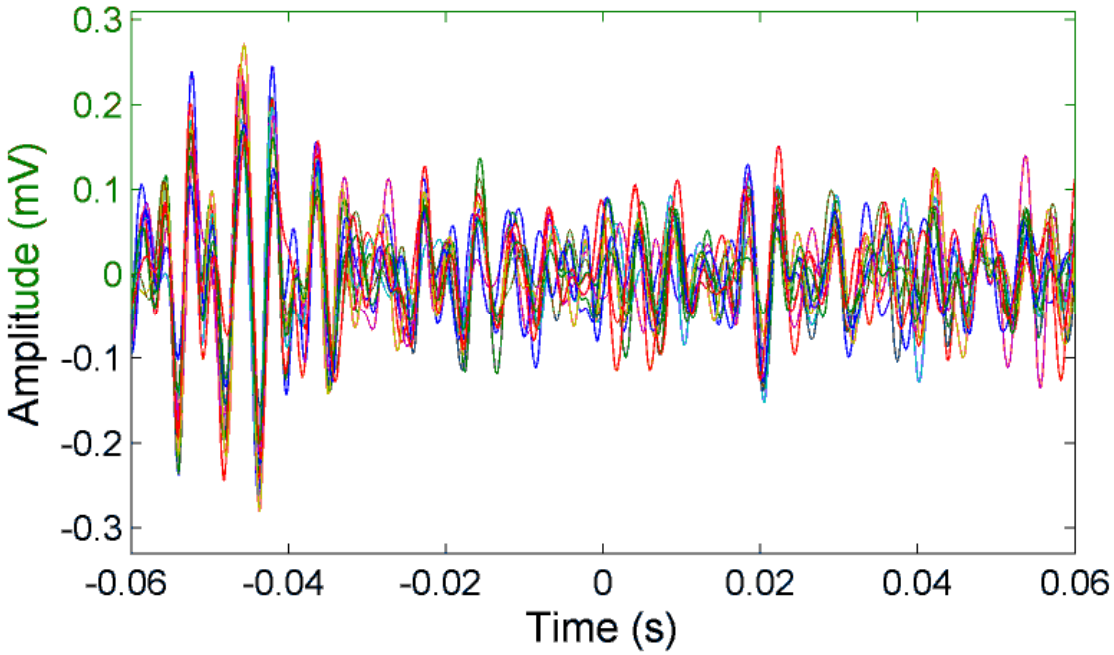

Figure 2.2. Representative multi-channel cerebellar signals plotted (only 16 channels for clarity) around the time of lever press (t=0). Signals are filtered between 150-350Hz to show the frequency band of interest. Multi-channel signals go in and out of synchrony episodically.

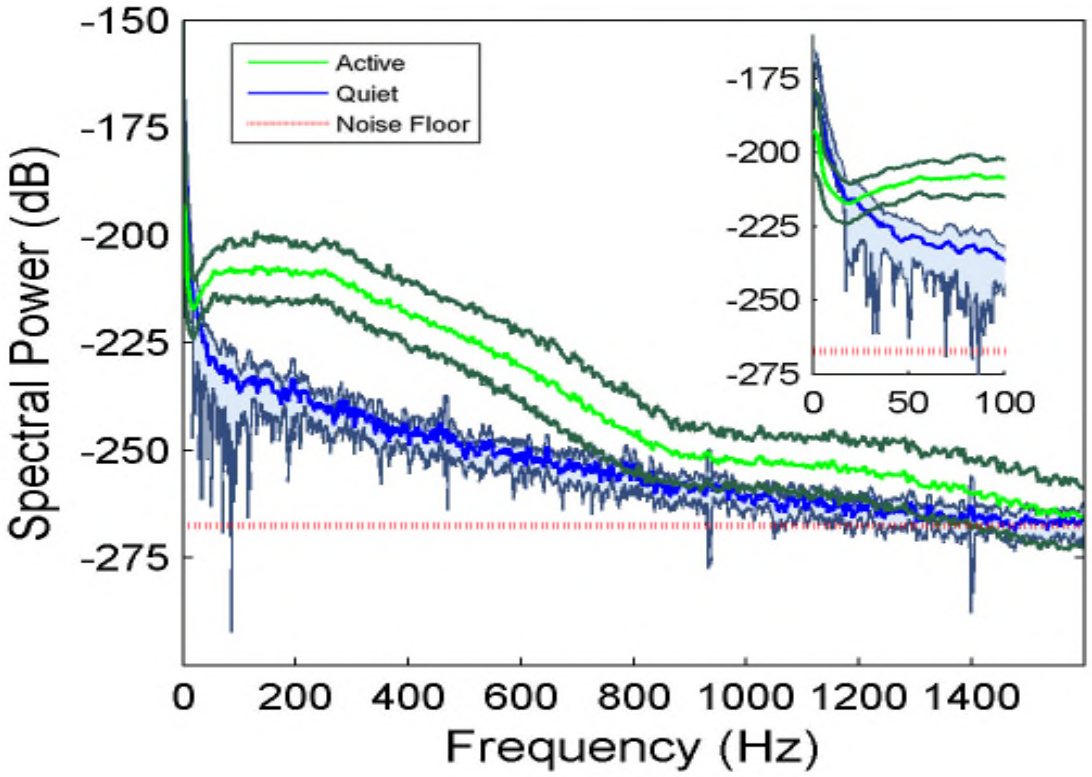

Figure 2.3. Average power spectra of the cerebellar signals collected from a rat during active behavior involving the forelimbs (N= 42 trials of 5 s recordings) and quietly resting (N=5 trials) episodes in the same recording sessions. Shaded areas indicate standard deviations. There is a large difference between the active and quietly resting states especially below 900 Hz. The red line indicates the estimated noise floor above which the signal power is considered to be from neural origin.

The inter-contact coherence during lever press (active in Figure 2.4) had near maximum values for the entire range of frequencies where there was neural signal power. The fact that coherence was high even at high frequencies where the signal power was very small (>900 Hz) suggests similar temporal signal patterns between recording channels at millisecond resolution. The coherence plots of the so called quiet episodes had varying amplitudes depending on the state of the animal that we were not able to judge visually, but in general they were much smaller compared to the active case at all frequencies. The quiet spectra had distinct peaks when the coherence values became

lower as observed in animal two (bottom plot in Figure 2.4). Those peaks above 900 Hz must be artifacts produced by the coherence function between very small amplitude noisy signals. The peak between 100-200 Hz, however, represents converging of neural signals into a narrower band during the resting state of the animal.

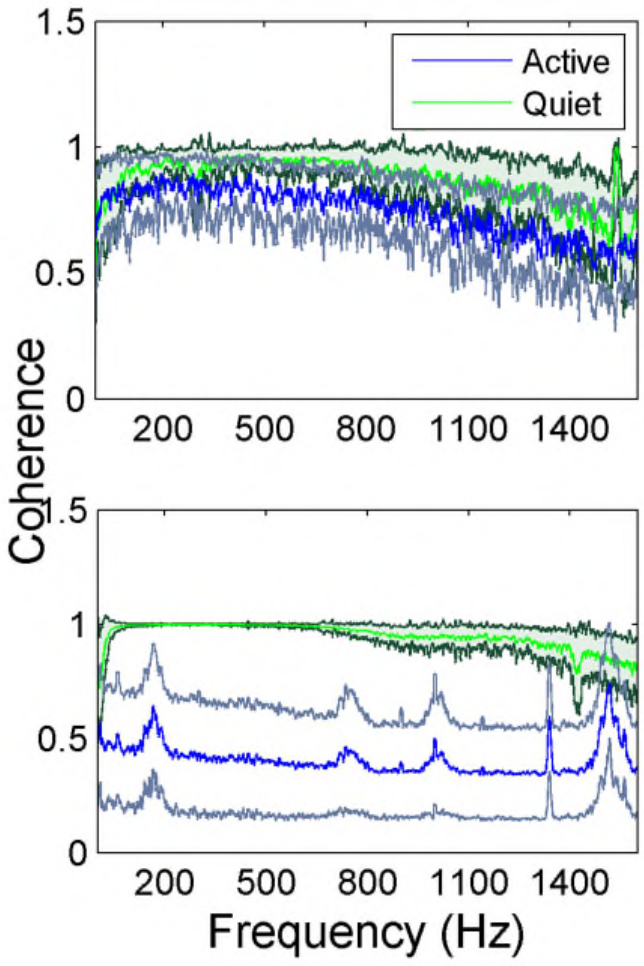

Figure 2.4. Average coherence between all channel pairs in the electrode array in two rats while the animals are performing lever press. In animal 1 (top figure) the green trace (dark green standard deviation) represents the coherence during the lever press task and the blue trace (grey standard deviation) is the quiet state (a total of N=42 trials for lever press and N=5 trials for the quiet state). Animal 2 (bottom figure) the green trace (dark green standard deviation) represents the coherence during the lever press task and the blue trace (grey standard deviation) is the quiet state (a total of N=23 trials for lever press and N=5 trials for the quiet state). The small peaks at higher frequencies are most likely artifacts produced by the coherence function between very small amplitude noisy signals.

The coherogram method was employed to determine how the inter-channel coherences varied as a function of time. The coherogram plot (Figure 2.5) demonstrated broadening of the frequency band and increasing in strength just before the lever press (around t= -0.2s). After the initiation of the lever press (t=0), there was a drop in

coherence followed by a slight increase again. There is also a peak of coherence in the beta band (~24Hz, green stripe) that follows a similar temporal trend with the high frequency band coherence (plots to the right in Figure 2.5). The correlation between the mean values of the 24Hz and 200Hz coherence plots as a function of time within t=±0.6 s suggests a high degree of similarity (R=0.70, 0.55, and 0.72 for animals 1-3 respectively). Based on the coherograms in Figure 2.5, we focused the synchrony analysis into the 150-350 Hz frequency band where the highest coherence values were detected before and after the behavior.

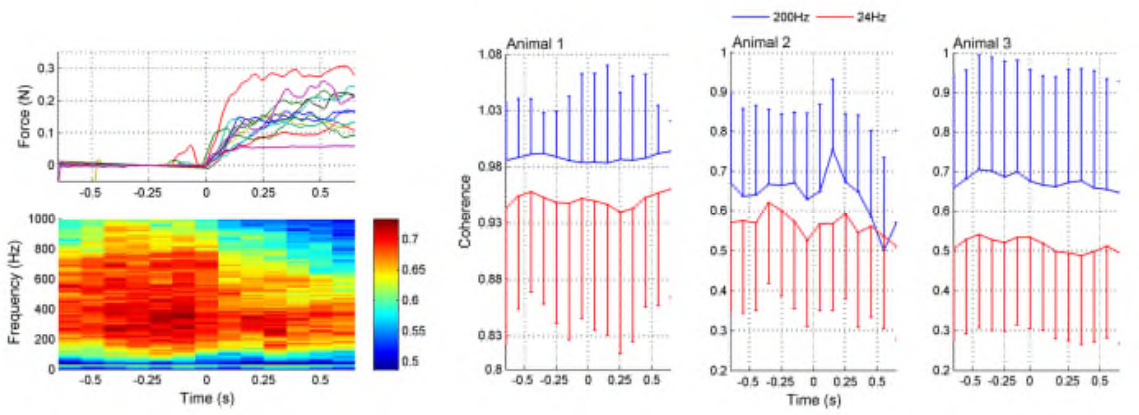

Figure 2.5. Coherogram data during lever press. Upper left plot: Representative force traces applied to the lever by the rat's forearm. Only a subset of the trials are plotted for clarity. The lever press takes place while the force is increasing and then the forearm rests on the lever while it is arrested at a fixed position by the computer. Lower left plot: Average coherence between all channel pairs in multiple trials (N=42 trials from three rats) as a function of time in a 200ms window leaping in 100ms steps. There is a peak in the lower band around 24 Hz. The high band extends from about 100 Hz to 800 Hz, though the maximum power levels during the movement, initiated at 0s, is found between 200 Hz to 350 Hz. Right plots (Animals 1-3): Coherence values specifically at 24Hz and 200Hz as a function of time. The mean and std are shown at both frequencies from the same trials (N=42, 23, and 18 trials in animals 1-3 respectively). Either positive or negative std is not shown in each plot for clarity.

The average synchrony plot from multiple trials in each animal (Figure 2.6) showed that there were alternating bands of high and low synchrony in time. There was a great deal of similarity between all three animals in temporal variation of synchrony values around the time of lever press. In all animals, a period of high synchrony occurred just before the initiation of the lever press. At the time of lever press initiation (t=0), there was a drop in synchrony followed by an increase again, similar to the trend in signal power. The times of second peaks in synchrony after lever press initiation closely correlated with transition times in the lever force plot from rising to plateau.

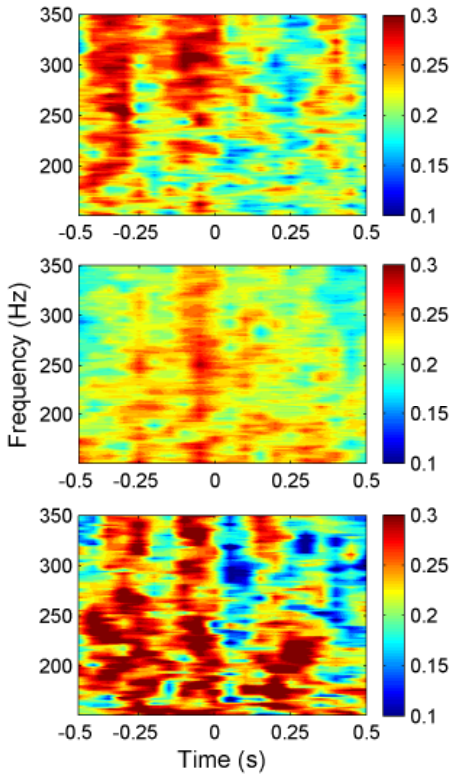

Figure 2.6. Synchrony values plotted as a heat plot within the frequency band of interest (150- 350 Hz) as a function of time for all three animals (N=42, 23, and 18 trials top to bottom respectively) showing a consistent pattern of synchronization between animals around the time of lever press. The pattern shows an increase in synchronization just before the movement, then a sharp decrease at the initiation of the lever press (t=0). Note that the alternating bands of high and low synchrony exist with or without behavior outside the time window shown.

The plots in Figure 2.7 were obtained by merging the amplitudes of synchrony values across all the frequencies within the entire band of 150-350Hz from multiple trials in each animal. The similarity between the temporal trends in synchrony in different subjects was indicated by a high average correlation of 0.65±0.18 within ±0.2s calculated between all animal pairs (N=3). In particular, the synchrony was completely disrupted at the time of movement initiation at t=0, i.e. the moment the hand touches the lever. ANOVA analysis showed a significant difference between the synchrony values for pre

(t=-0.1) and post (t=0.1) initiation of the lever press (α=0.01). There was no significant difference between Animal 1 and Animal 2, however, Animal 3 was significantly different from both in terms of average synchrony values (α=0.01).

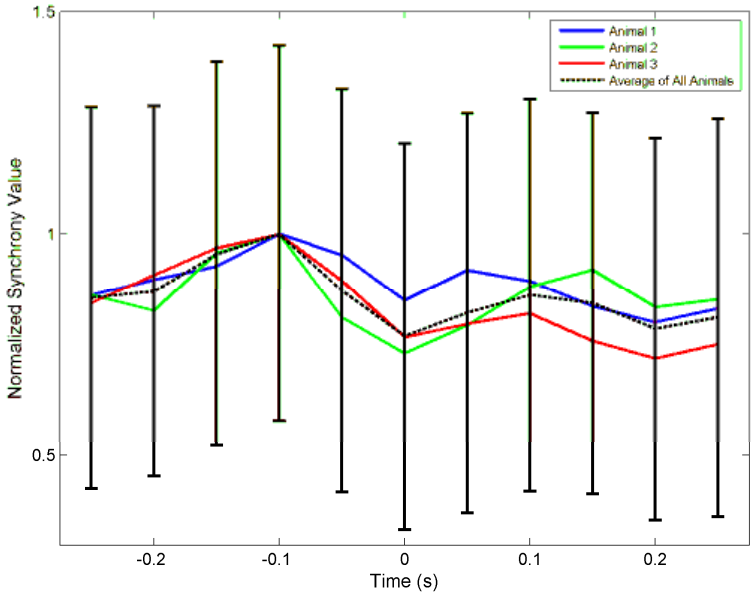

Figure 2.7. Synchrony values were averaged across 150-350 Hz band, normalized to eliminate inter-contact variations, and averaged across contacts and trials in each animal (N=42, 23, and 18 trials in animals 1-3, respectively). The synchronization pattern is similar in all three animals around the time of movement initiation. Bars indicate overall standard deviation of group data from all animals. The average correlation of these time plots between animals is 0.65±0.18 within the time interval of ±0.2 s.

Next, the spatial distribution of phase synchrony over the recording area was analyzed. An example of the synchrony for each contact in the array with respect to a reference contact (red square) is shown in Figure 2.8. In all animals, synchrony could be seen spread over the entire cortical area covered by the electrode array. The highest synchrony was observed generally with contacts near the reference contact against which all the synchrony values were computed. However, not all the contacts next to the reference showed high synchrony. The synchrony values did not vary monotonously by

distance as it would be expected if the synchrony was due to a distant common source, e.g. cortical cells in deep sulci or deep cerebellar nuclei. Therefore, it was inferred that the synchrony between the recording channels emerged from the cortical neurons beneath the electrode and not from a distant, common mode signal.

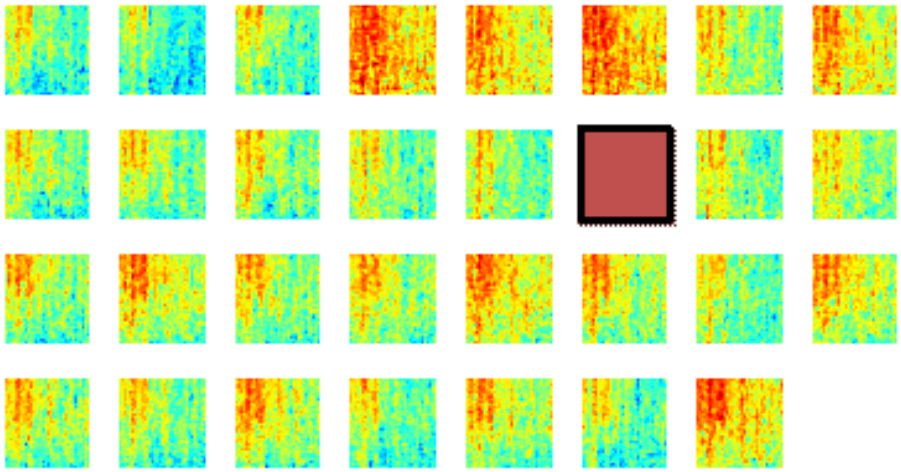

Figure 2.8. Phase synchronies between a reference contact (brown square) and all the others in one rat during multiple lever pressing trials (N= 40). These plots show that the synchronization spread over the entire area covered by the array, although the highest synchrony values are to be found near the reference contact. Synchrony values are not monotonously decreasing with distance from the reference electrode. The X-Y axes for each mini plot are same as in Figure 2.6. A channel is missing at the corner because of one less count on the number of amplifier channels.

In order to investigate if some contacts synchronized and followed a similar synchrony trend in time as a group, we applied the clustering analysis to the synchrony values from each contact (or recording channel) as a function of time (see Methods). The clustering of contacts from two different animals is presented in Figure 2.9. The plots represent the two largest clusters for each animal where the membership strengths (SM)

are color coded. The contacts within the same group are contiguous in the bottom plot but not in the top (blue group is divided). There does not appear to be any directional orientation in synchrony in these maps. A statistical analysis, however, suggests slightly higher synchrony values in the medio-lateral direction (Figure 2.10). This analysis also clearly demonstrates that the synchrony values decrease very slowly as a function of inter-contact distance.

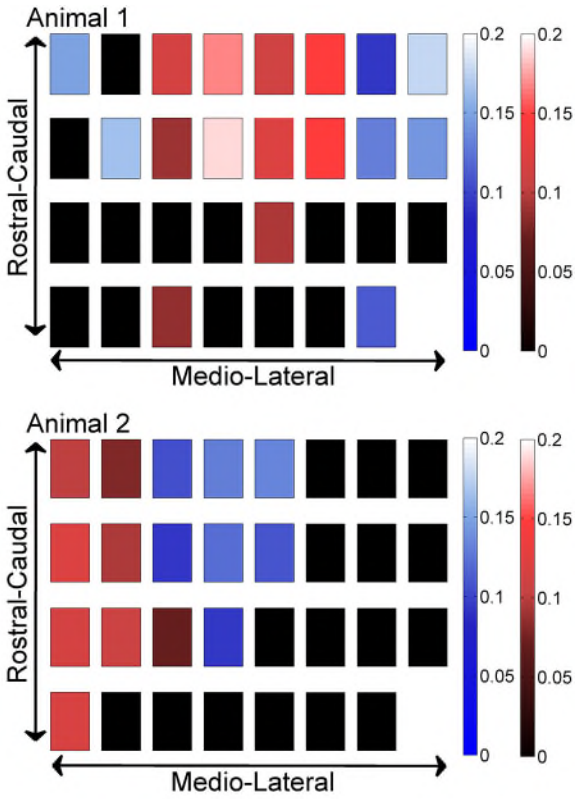

Figure 2.9. Clustering of contacts by synchrony in two different animals (N=42 and 23 trials), with each square representing an electrode contact. The two largest clusters are marked by two different contact colors (red and blue) in each animal. The color gradients represent the strength of membership (SM) for each contact to its own group. The smaller the value, the weaker the membership. The groups present a patchy spatial organization across the PML cortex, rather than parasagittal zones.

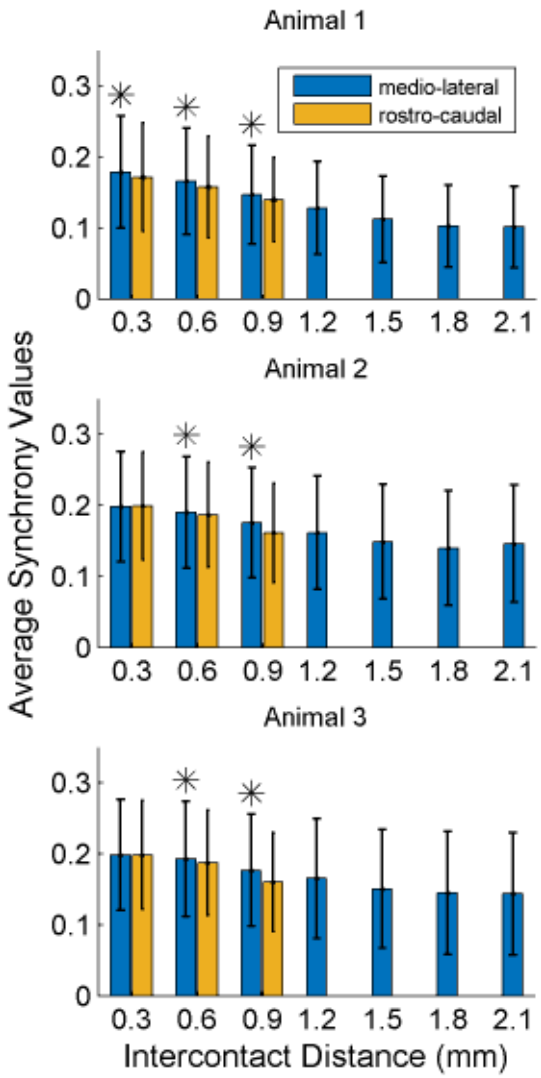

Figure 2.10. Synchrony values as a function of inter-contact distance and orientation. The synchrony on average decreases slightly by distance in both directions. Medio-laterally oriented contacts (in blue) have a slightly higher (* significance, $p<0.01$) synchrony than rostra-caudal ones (yellow) for inter-contact distances of 0.6 and 0.9 mm in all three animals, and also for 0.3 mm in the first rat. Other inter-contact separations in the rostra-caudal direction are not available for comparison. The number of trials in each animal are the same as in Figure 2.8.

2.1.3 Discussion

The lever pressing task was chosen because it provided a non-cyclic, stereotypical behavior that presumably involved the cerebellum and the PML in particular. Difficulty arises in interpretation of neural signals collected during cyclic motor tasks in terms of their temporal relation to the behavior, such as face cleaning. Lever pressing task has been shown to give rise to high frequency oscillatory activity in the cerebellum (Oehler, Pickenhain et al. 1969).

We can only speculate about the source of the neural signals recorded from the cerebellar surface. The single spike activity of the Purkinje cells is estimated to have the largest share in the signals due to their proximity to the surface, although granular cells and their ascending axons may be contributing as well. Our results on coherence and synchrony are in agreement with those reports on characteristics of Purkinje simple spike activity recorded with indwelling electrodes, as discussed below. Parallel fiber action potentials cannot be considered as a significant source for surface field potentials because of large variability in their times of arrival under each electrode contact and thereby making their constructive superposition highly unlikely. The post synaptic potentials of the Purkinje dendrites and mossy fiber terminals can also be ruled out as a major source due to the low frequency content of their activity compared to the somatic spikes.

We first investigated the amplitude modulation of the high frequency oscillations during the lever press task. The analysis showed that the high frequency oscillations (150-350Hz) increased in power before the lever press, decreased during the lever press, and increased again after the lever press was completed. This temporal trend of neural activity in relation to a motor function is in agreement with reports on Purkinje cell single

spike activity. Abrupt changes in simple spike frequency at the time of rat's hand touching the food pellet were reported from the on-beam and off-beam Purkinje cells of the PML (Heck, Thach et al. 2007). Purkinje cell spike frequencies also increased during forelimb swing compared to the stance phases of walking in cats (Armstrong and Edgley 1984). Similarly, in rhesus monkeys, the Purkinje cells increased their firing rates during brief, cue-initiated movements (Thach 1970, Thach 1970).

Interestingly, our coherence analysis also indicated that there were similar trends in the high frequency coherence and the beta band coherence amplitudes in relation to the lever press. This trend of high frequency band coherence time-locked to the behavior was similar to that of 4-25Hz band signals of the cerebellar cortex, which have been shown to emanate from the granule layer (Pellerin and Lamarre 1997, Courtemanche, Pellerin et al. 2002). This suggests that the granule layer oscillations and the high frequency oscillations observed from the pial surface in this study may be related. Beta band oscillations of the cerebellum and that of the motor cortex were coherent during sustained movements in monkeys (Soteropoulos and Baker 2006).

Temporal analysis showed alternating bands of high and low inter-contact phase synchrony throughout the recording episodes. There was a consistent pattern in synchrony that was time-locked to the moment of lever press across all trials. The inter-contact synchrony values peaked just before the movement, took a sharp decline at the time of lever press, and presented a smaller peak after the lever press was completed. This pattern was reproducible in all three animals. These results strongly argue that the spatiotemporal synchrony in the high frequencies (150-350Hz) of the PML field potentials are related to the forelimb behavior. The heightened simple spike synchrony

for a few hundred milliseconds before the hand touching the food pellet was interpreted as the involvement of the PML in reaching behavior (Heck, Thach et al. 2007). This type of zero-lag simple-spike synchrony was significantly higher in the medio-lateral direction along the parallel fibers (on-beam) compared to the rostra-caudal (off-beam) orientation of the recording electrodes at 305μm and 610 μm contact separations. The spatial extent of the field potential synchrony reported here is much larger than what was seen in the synchronization of Purkinje cell single spike activity and only slightly dependent on direction. In many studies under several different anesthetic regimens Purkinje cell single spike synchrony (~1ms) was found between cells separated by less than 100 μm (Bell and Grimm 1969) (MacKay and Murphy 1976, Ebner and Bloedel 1981) (De Zeeuw, Koekkoek et al. 1997, Shin and De Schutter 2006). Others have reported synchronizations up to a few hundred micrometers and quickly decreasing by distance (Heck, Thach et al. 2007, de Solages, Szapiro et al. 2008). The field potential phase synchrony measures reported here spread across the entire electrode array (0.9 x 2.1 mm) and did not show a strong dependency on distance. Such a large scale synchrony, clearly detectable as a field potential in the PML must be representing a more global and perhaps centrally driven state, such as an elevated level of attentiveness, rather than encoding a specific behavior. Our results do not argue against the factors that may be responsible for simple spike synchrony. Instead, there may be two different mechanisms playing a role at two different scales; axon collaterals augmenting the micro scale synchrony at distances of a few hundred micrometers (Heck, Thach et al. 2007, de Solages, Szapiro et al. 2008) and the mossy fiber inputs modulating this synchrony at larger scales as seen in this study.

The clustering analysis showed only a slight directional preference in spatial distribution of synchrony. The size and location of the synchronized areas are consistent with the patchy organization of the granule layer to tactile stimulation, as originally reported by W. Welker's lab (Shambes, Gibson et al. 1978), rather than the parasagittal zones formed by the climbing fiber system. The size of the cortical area investigated was still small to observe multiple patches within the same group of synchronized contacts. It was originally hypothesized by Llinás that ascending segments of granular cell axons preferentially terminate on the superjacent Purkinje cell dendrites (Llinás 1982). Ekerot and Jorntell found that the receptive fields of Purkinje cells corresponded to that of the mossy fiber terminal aggregates rather in neighboring microzones (Ekerot and Jorntell 2003). The microzonal relation was preserved more strictly between the receptive fields of the mossy fiber terminal aggregates and the molecular layer interneurons. Thus, considering these reports collectively there may be a modulation effect of the Purkinje simple spike activity within a cortical area by the granular cells subjacent roughly to the same area, even though this spatial correspondence may not be at the resolution of individual microzones.

Finally, we speculate that the sharp drop in synchrony at the time the rat's hand touches the lever must be due to the stimulation of the cutaneous mechanoreceptors. It has been argued that the peripheral inputs entrain and synchronize the Purkinje simple spikes and thereby modulate the output of the deep cerebellar nuclei (see (Person and Raman 2012) for review). That is, higher synchrony is associated with increased cerebellar output. Again these seemingly controversial ideas can be reconciled by making a distinction between simple spike synchrony of local Purkinje cells and the large

scale synchrony of the field potentials recorded in this study. The cutaneous inputs must be entraining various subpopulations of Purkinje cells at different frequencies and therefore, desynchronizing these groups of cells from each other whereas they are all driven at the same frequency before the stimulus by a common input through the mossy fiber system. This is supported by the fact that the coherence spectra had a distinct peak at ~100-200Hz in a quietly resting animal which was replaced by a wider spread high coherence values during activity. A slight broadening of the field potential spectral peak was observed in the awake rat cerebellum as compared to anesthetized preparations (de Solages, 2008). Our large scale synchrony looks like a characteristic of a global brain state, e.g. attentiveness or preparation for movement, rather than encoding of a specific motor behavior. An alternatively explanation is that the entire musculature of the ipsilateral forelimb may be contracting during the reaching behavior, which may be encoded by the observed synchrony within a large cortical area dedicated to the entire forelimb in the PML. In conclusion, further investigation is needed to shed light on how the peripheral sensory and central command information interact at the cerebellar cortex during behavior and if this interaction can be explored with spatiotemporal synchrony patterns of high frequency oscillations in the cerebellar cortex.

2.2 Low Frequency Oscillations and Relationship to the High Frequency Potentials

Oscillations form an integral part of neural processing. They are believed to form the basis for complex temporal patterns which allow multiple areas of the brain to function together (Buzsáki and Draguhn 2004, Buzsaki 2006). The oscillation bands in the 4-30Hz have been shown to be present in a number of cortical and subcortical structures and are significant in an number of areas including learning, memory, motor control, and sensory integration (Murthy and Fetz 1992, Sanes and Donoghue 1993, Pesaran, Pezaris et al. 2002, Jensen, Goel et al. 2005, Lee, Simpson et al. 2005, Benchenane, Tiesinga et al. 2011, Ronnqvist, McAllister et al. 2013, Picazio, Veniero et al. 2014). It was once thought the cerebellum did not contain these oscillations, however it has been now documented that these oscillations are pressent in the cerebellum as well (Pellerin and Lamarre 1997, Hartmann and Bower 1998).

These oscillations have been shown to originate from both the granule layer and the inferior olive (Pellerin and Lamarre 1997, Hartmann and Bower 1998). The granule layer oscillations appear as a spindle shaped waveform (Pellerin and Lamarre 1997, Hartmann and Bower 1998). These oscillations are synchronous across the lobule and even in the contralateral lobule (Hartmann and Bower 1998). They are best recorded when the animal is showing little or no movement and are stoped by the initiation of the movement (Pellerin and Lamarre 1997, Hartmann and Bower 1998). They do not however, predict the movement given that the oscillations can be pressent and then stop when no movement is pressent (Hartmann and Bower 1998). The oscillations are most related to a state of attention or expectancy (Pellerin and Lamarre 1997, Hartmann and Bower 1998). These oscillations originate from the granule layer and are most related to

the granule cell multi-unit activity (Courtemanche, Pellerin et al. 2002). They have also been shown to have a relationship to the Purkinje cell simple spike activity (Courtemanche, Pellerin et al. 2002, Lu, Hartmann et al. 2005). These oscillations show a parasagital orientation in the synchrony of the granule layer oscillations (Courtemanche, Chabaud et al. 2009). This synchrony is expanded into the coronal orientation during active expectancy (Courtemanche, Chabaud et al. 2009).

The 4-25 Hz oscillations in the granule layer have also been found to be synchronous with the cortical oscillations in the same frequency range (Courtemanche and Lamarre 2005). The primary somatosensory cortex (S1) showed the highest synchrony with the primary motor cortex showing a presant but weaker synchrony (Courtemanche and Lamarre 2005). This synchrony was highest while the animal was in a high state of attention waiting to make a movement while showing a weaker synchrony while the animal was waiting on a food reward (Courtemanche and Lamarre 2005). The S1 synchronies showed a hand dominance in the synchronies with the hand ipsilateral to the cerebellum showing the highest synchrony. The M1 synchronies showed no dominance (Courtemanche and Lamarre 2005).

The inferior olive were first discovered under the influence of haraline which increases the subthreshold osccilations to super threshold causing a highly coherent 10Hz spiking of the inferior olive cells (Lamarre, de Montigny et al. 1971, De Montigny and Lamarre 1973). These oscillations normally appear as subthreshold oscillations ranging from 1-7Hz (Devor and Yarom 2002, Chorev, Yarom et al. 2007). Olive cells are connected through gap juctions (Llinas, Baker et al. 1974) causing them to oscillate in groups (Leznik, Makarenko et al. 2002). The resulting climing fibers show a hightened

synchrony in the parasagital direction (Lang, Sugihara et al. 1999). This lines up well with the parasagital distribution of climbing fiber lining up with the zebrin bands (Voogd, Pardoe et al. 2003, Voogd and Ruigrok 2004).

The objective of this aim is to relate the low frequency field potentials to the movement and the high frequency field potentials in the cerebellum and to compare the field potentials to the cerebral potentials. The results show an increase in synchrony of the low 10-15Hz potentials during the action of pressing the lever. This is opposite to the synchrony in the high frequencies 150-350Hz which show a high synchrony before and after the pressing of the lever. There is also shown to be a synchrony between the motor cortex and the cerebellum in the 10-15Hz or 4-9Hz range immediately before the initiation of the lever press. The stimulation of the motor cortex results in an increase of the high frequency amplitudes with a resonance peak at 7Hz**.** The results obtained in the following section were obtained using the same methods found in Section 2.1.1.

2.2.1 Results

The signals recorded during a lever press task with a food reward while the animals were allowed to move freely during the movement and given a five second period with which to press the lever are presented in Figure 2.14. Figure 2.11 shows several examples of low frequency signals with the vertical force profile. The signals show, at the initiation of the movement a decrease of the amplitude of the oscillation. In some examples this decrease continues for the duration of the movement, however, this is not the case in all observations.

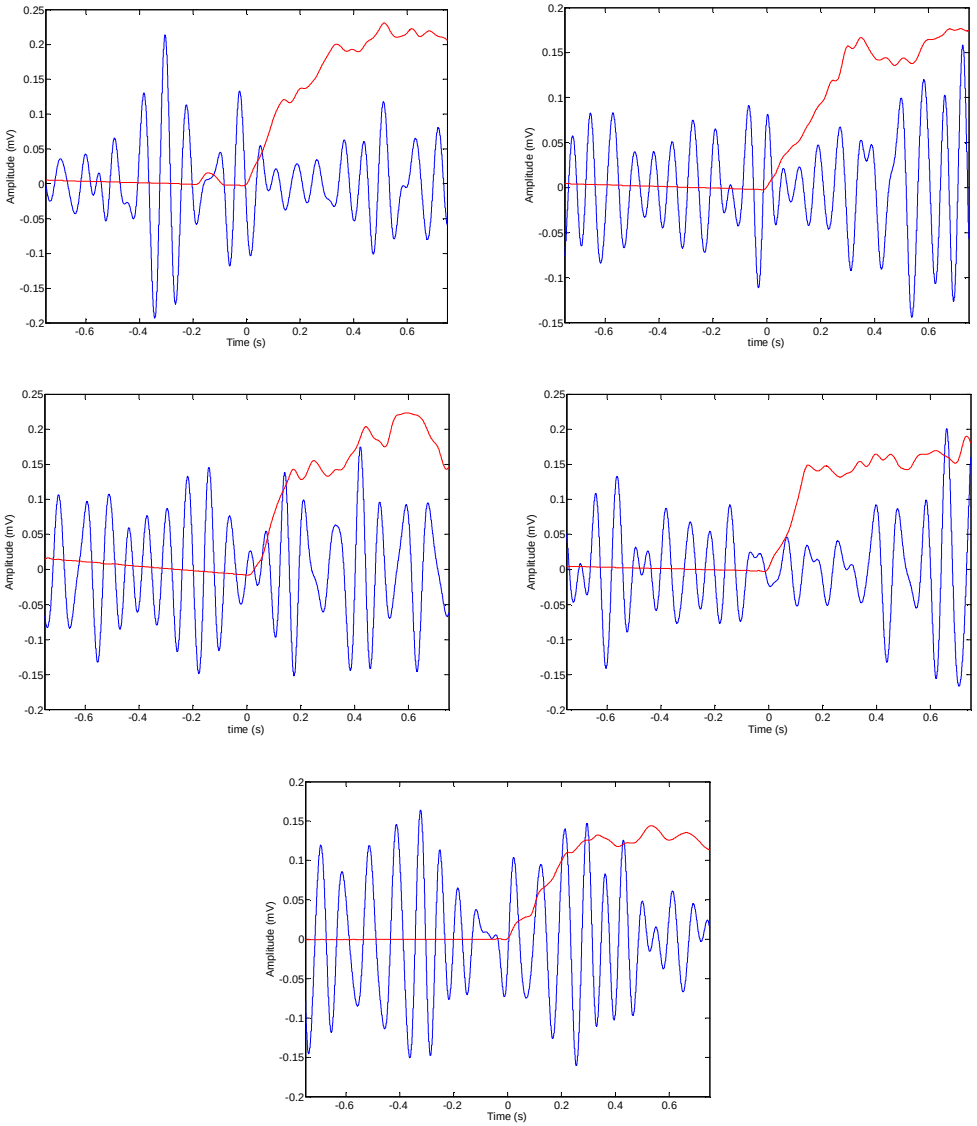

Figure 2.11 10-15Hz oscillations (blue) with force profile (red) before and during a leverpress task for various trials. The figures show a decrease in the amplitude at the initiation of the lever press. Some show a sustained decrease in amplitude however, this is not seen in all trials.

The coherence between contacts in the low freqeuncy range was observed during the lever press task. Figure 2.12 shows the coherogram in the 2 to 50Hz range with zero marking the initiation of the lever press. The results show that there is a peak in the coherence at 24Hz. It also shows that the coherence is strong just before the initiation of the lever press. The coherence then drops during the movement and increases after the

movement. There is a similar pattern for the lower frequencies however, there is a much lower coherence.

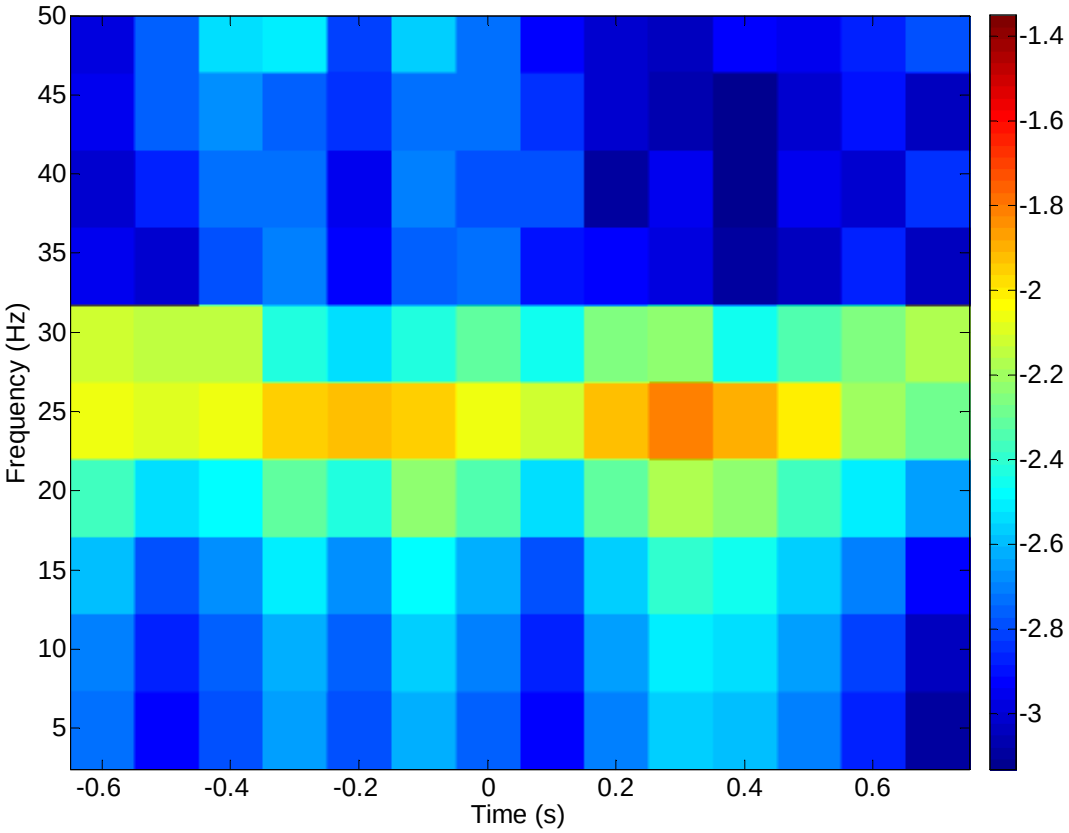

Figure 2.12 Average coherogram between all channel pairs in multiple trials (N=42) using the multitaper method. Figure shows a peak coherence in the ~24Hz band. The coherence increases immidiately before the movement and decreases at the initiation of the lever, then increase again.

The correlations between the high frequency and low frequency coherence show a large similarity in their profiles. Figure 2.13 shows the time profiles of the coherence for 200Hz (red) and 24Hz (blue) for two different animals. Both traces show an increase in the coherence before the lever press, followed by a decrease, then an increase after the

press. The average correlation coefficient for the plots is 0.6, between the coherences for the two frequencies.

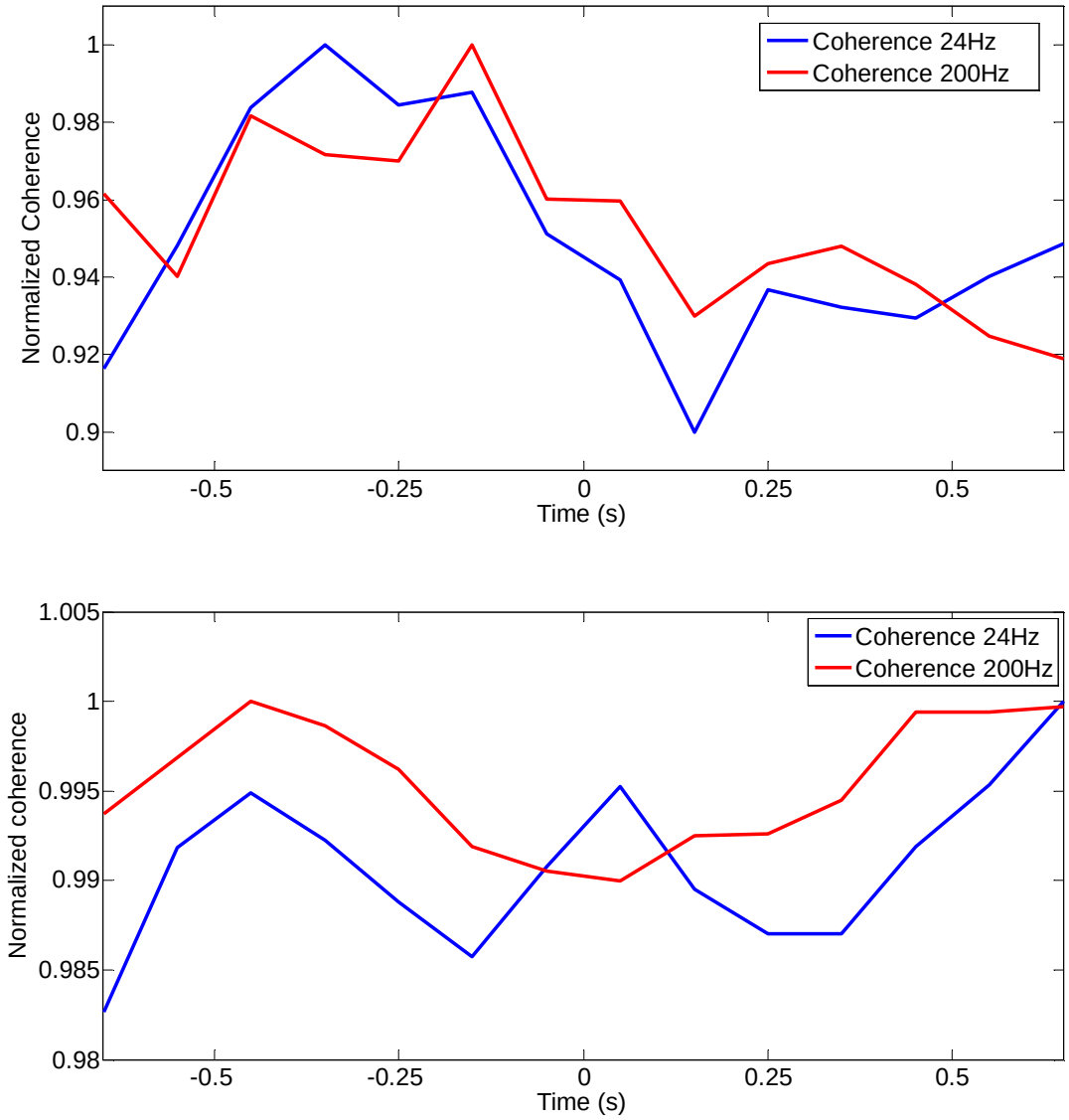

Figure 2.13 Time plots of the coherence at 24Hz and 200Hz for two animals. Both show a decrease in coherence around the initiation of the lever press and an increase after. The correlation between the 24Hz and 200Hz coherences is 0.68 and 0.52 respectively.

Based on the coherence, the phase synchrony was calculated from 2 to 32Hz during the lever press. The synchrony of the lower frequency potentials (Figure 2.14)

showed a lower value of synchrony than the high frequency potentials. The results show that there are distinct bands of synchrony in the 3-5Hz, 10-15Hz, and 22-27Hz ranges in all animals. Unlike the coherence at 24Hz band that does not show the largest synchrony, rather it is the 10 to 15Hz band that shows the greatest synchrony. The only band to showed consistant modulation with the movement was the 10-15Hz band. This band showed an increase in synchrony after the initiation of the lever press and maintained it through the time of movement. This is in sharp contrast to the synchronies in the 150-350Hz range wich showed an increase in synchrony before and after the movement of the lever and a decrease during the lever press.

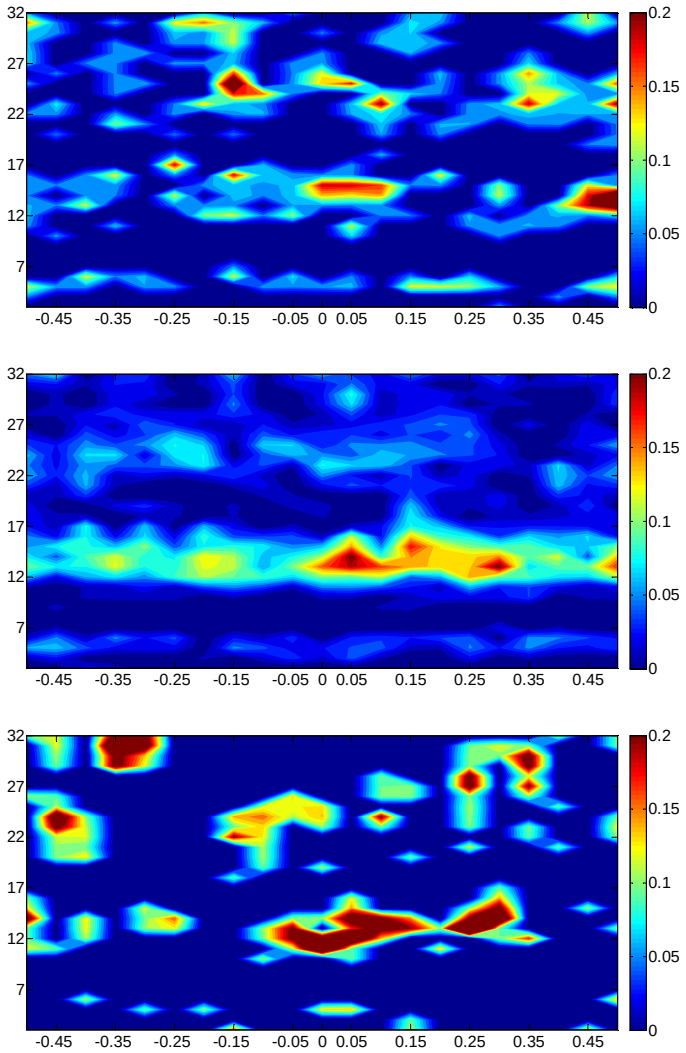

Figure 2.14 Average intracerebellar synchrony plotted over time for three different animals (N=42, 23, 18 respectively) showing a consistent pattern of synchronization between animals. The pattern also shows an increase in synchronization just after the movement is initiated (t=0) and extends during the movement of the lever.

The spatial analysis showed that synchrony was pressent across the entire recording space. Figure 2.15 shows a representation of the synchrony aross the electrode recordings with each plot representing an electrode. This is similar to the results shown in the high frequency analysis. The synchronies do not seem to be consistant with a pure volume conduction from a distant source. The area of high synchrony in the low and high frequencies though similar do not match up contact to contact.

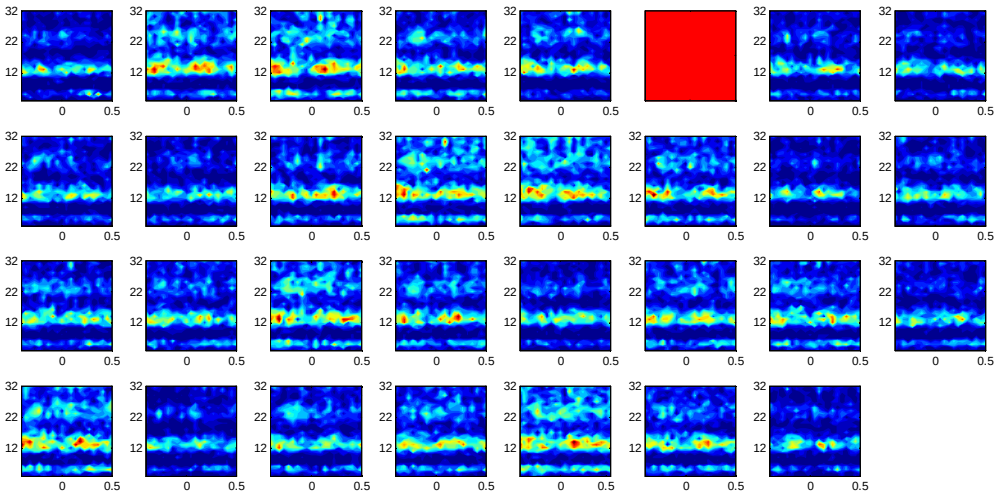

Figure 2.15 Synchronizations between a reference contact (red square) and all the others in one rat during multiple lever pressing trials (N= 40). These plots show that the synchronization spread over the entire surface of the array, however, the highest synchronization is located around the reference contact. This also shows that the synchronization is not monotonously decreasing with distance from the reference electrode and therefore, synchrony is not due to volume conduction. The X-Y axes for each mini plot is same as in Figure 2.12.

Next we observed the synchrony between the motor cortex and the cerebellum (Figure 2.16). The cerebro-cerebellar synchrony is much more limited in the bandwidth than the intracerebellar synchrony. Two of the animals show synchrony in the 10-15Hz band similar to the intracerebellar synchronies, the third animal shows synchrony in the 5-9Hz band. Even though the frequencies do not match the timing of the synchronies are similar. The synchrony begins ~150-70ms before the movement and ends just after the initiation of the lever press. There is also a consistant synchrony 350-450ms before the initiation of the lever press. The timing of the cerebro-cerebellar synchrony therefore, precedes the intracerebellar synchrony.

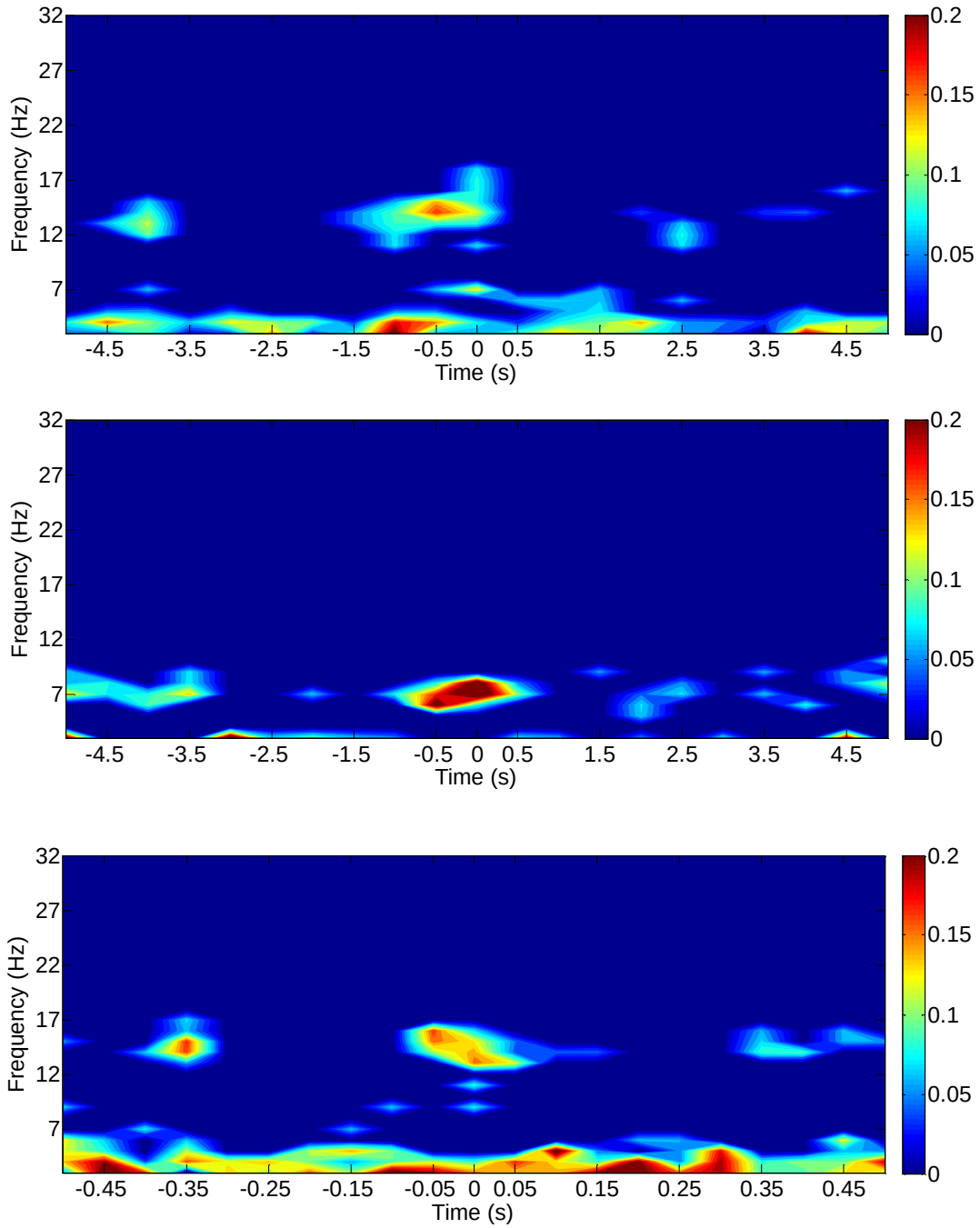

Figure 2.16. Average cerebro-cerebellar synchrony plotted over time for three different animals (N=42, 23, 18 respectively) showing a consistent pattern of synchronization between animals. The pattern also shows an increase in synchronization just after the movement is initiated (t=0) and extends during the movement of the lever.

In order to determine if the high frequency potentials could be modulated by the low frequency oscillations, we stimulated the motor cortex using pulse trains at

frequencies ranging from 5 to 10Hz. The means of the signal standard deviation for each frequency (figure 2.17) show a bell curve like profile with a peak around 7Hz. This analyis was done in the same animal that showed a 5-9Hz synchrony between the motor cortex and the cerebellum which also showd a peak synchrony at around 7Hz.

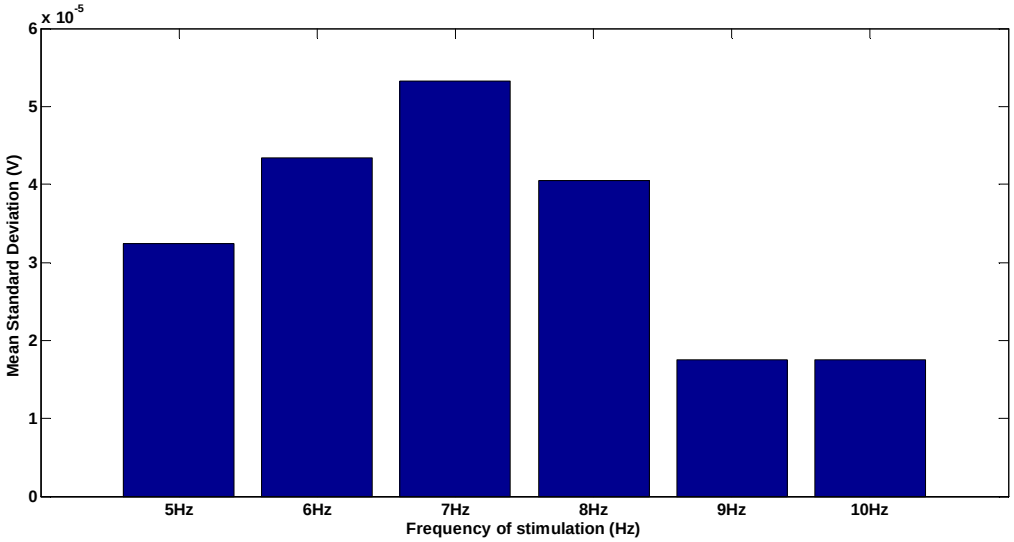

Figure 2.17. Amplitudes of the Very High Frequency Oscillations vs. the frequency of stimulation applied to the primary motor cortex. This shows that there is a resonance in the very high frequency oscillations with a peak at 7Hz. This is the same frequency seen in the synchronies between the cerebellum and the motor cortex in this animal.

2.2.2 Discussion

The results show that the low frequency signals reveal a decrease in amplitude at the initiation of the lever press. In some trials, this reduction in amplitude persists during the movement however, not in all trials. Despite the variability these results are consistant with the results seen in previous studies (Pellerin and Lamarre 1997, Hartmann and Bower 1998, Courtemanche, Pellerin et al. 2002). The variability seen in the current results is most likely due to the slight changes of the implant site in each animal.

The coherence analyisis of the low frequency potentials show a peak coherence at ~24Hz. This coherence shows a similar modulation to the high frequency coherence. The phase synchrony shows a peak synchrony in the 10-15Hz range. The phase synchrony in the 22-27Hz was present, however, it showed a lower synchrony compared to the 10-15Hz range. The modulation of the 22-27Hz range also showed less consistant modulation with the movement in the synchrony analysis.

The 10-15Hz synchrony showed a different modulation to the high frequency synchrony, being synchronous during the pushing of the lever press. While the high frequencies were synchronous before the initiation of the lever press, and it decreased at the initiation of the lever press, the low frequencies show a low or no synchrony before the initiation and a high synchrony during the lever press.

The spatial distribution of the synchrony showed a broad distribution of the synchony, extending the entire length of the array. The synchrony did not show a decreasing trend with distance from the electrode, which would be indicative of volume conduction; rather there were high sychrony contacts distant from the reference and lower synchrony contacts near the reference which is indicative of the synchrony being due to the underlying neural activity. This broad synchrony is similar to those reported by other groups who have shown that the granule layer oscillations present a broad range of synchrony within lobules and even shown to be synchronous across hemispheres of the cerebellum.

The cerebro-cerebellar analysis indicated synchrony in the 10-15Hz band for two animals and 5-9Hz in the third. The 10-15Hz synchronies are in the same range as those seen in the intracerebellar ones. While the frequencies were different, the temporal

pattern of synchrony was the same for all three animals with respect to the lever press. The synchrony increases before the movement and peaks just before the initiation of the lever press. This synchrony profile is consistant with the Mu band profile of activation that increased in amplitude just before movement and decreased during the movement (Sanes and Donoghue 1993, Donoghue, Sanes et al. 1998).

The stimulation analysis demonstrated that stimulation of the motor cortex in the Theta band does elevate the amplitude of the high frequency potentials in the cerebellum. The stimulations resulted in a peak amplitude of the high frequency potentials at 7Hz. This was performed in the same animal that showed high cerebro-cerebellar synchrony in the 5-9Hz band. This results suggest that there is a resonance of the high frequency potentials at 7Hz which matches the frequencies of sychrony between the motor cortex and the cerebellum.

2.3 Conclusions

The results demonstrate that the high frequency potentials are functionally related to the movement. It also suggests that these potentials may be related to the state of the animal. The high frequency signals reveal the highest degree of modulation during movements that include some level of expectancy and therefore, a higher level of attention. The potentials are shown to modulate the synchrony between contacts that spread over to ~2mm distance across the cerebellar surface. The high frequency potentials have a very broad bandwidth ranging from 150-800Hz. The entire range of frequencies tend to be modulated together. This pattern of broad high frequency potentials are thought to represent the spiking activity in the underlying cells.

The cerebellum represents a complication of how to interpret the field potentials particularly the cellular origin of the high frequency potentials. In the motor cortex only the pyramidal cells have a regular vertical axis whereas the other cells have a more random orientation. The vertical orientation is the best orientation for recording field potentials because it lines the dipole up without canceling itself out as the random orientated neurons do. This leads to the assumption that the majority of the variation in the field potentials recorded from the cerebral cortex comes from the pyramidal cells. The cerebellum, on the other hand, has a very regular cellular architecture. All the major cell types, Purkinje cells, climbing fibers and granule cell/ Golgi cells, are orientated in the vertical direction. Therefore, no such assumption of cell type can be made in the cerebellum. In order to determine the source of the field potentials recorded on the surface, a relationship of the field potential and the spiking activity of a particular cell group needs to be studied, or a penetrating electrode study need to be conducted to determine the depth of max field potentials and therefore, the cell type accounts for the greatest variation in the field potential. It can be assumed that the climbing fibers represent the least contributor to the overall variation because of the low frequency of their firing. The two primary sources for the field potentials are therefore, the granule cells and the Purkinje cells. There is early evidence that the high frequency potentials may be related to the 4-25Hz potentials, which have been shown to originate from the granular layer (Courtemanche, Pellerin et al. 2002, Lu, Hartmann et al. 2005). This still does not help to determine the origin of the potentials because the Purkinje cells have also been shown to be driven by these oscillations from the granular layer (Courtemanche, Pellerin et al. 2002, Lu, Hartmann et al. 2005).

More research needs to be done before the function of the high frequency potentials can be determined however, there are several possibilities. It is clear that the potentials are most likely due to the underlying spiking activity. The highest amplitudes will occur when large groups of cells are firing together. The more in phase firing the better, as out of phase bursts will cause a cancelation of the field. This spiking has to be in at least a moderately synchronous firing pattern as the high frequency potentials were highly synchronous over the entire electrode surface. One possibility is that the high frequency potentials are due to the burst firing that happens during the 4-25Hz oscillations in the granular layer. This idea has several implications. There is some early evidence that the two signals are related. The 4-25Hz oscillations have been shown to have a broad synchrony across the cerebellar cortex. The modulation of synchrony in the high frequency potentials is similar to the amplitude modulation of the 4-25Hz oscillation. While this project has shown some relationship of the high frequency potential to the movement, it is not clear yet if it is only related to movement or even if it is primarily related to movement as the high frequency potentials are present even when no movement is noticeable. Some preliminary evidence suggest that it may be related to the attention or expectation state of the animal. It seems that these potentials do not necessesaryly represent the kinematics or force of the animal's movement. The potentials could represent a preparation of movement as the high frequency potentials come to their highest synchrony just before the movement. It is also possible that these potentials could represent a sensory input as this was not well controlled for in this study. Much more research is needed for conclusively decide on the function of these potentials.

There are several uses of this research; the first and most obvious is to have a better understanding of the function of the cerebellum. By understanding the high frequency potentials, the large scale firing patterns of the underlying neurons can be better understood. Another implication can be the greater use of recordings from the cerebellum in clinical examinations. The cerebellum has a wide degree of functions that affect large portions of the brain, however, it is not as often used in clinical examinations. Part of this has been that the field potentials from the cerebellum have not been well described. This project furthers the understanding of these field potentials which may increase the importance of the cerebellum in clinical research. The field of brain-computer interfacing constitutes another application. The cerebellum receives large amounts of inputs from much of the cortex and therefore, can offer information about many different types of changes in the animal's state.

CHAPTER 3

FUTURE DIRECTIONS

The behavioral and training protocol need to be refined so that the resulting recordings can be better determined if they are from sensory or motor origin or due to an attentive state of the animal. The first area that should be improved is that the animal should not be free to move around the cage thus limiting the influence of walking and exploring the cage on the animal. The second area that needs to be refined is that the animal should be trained to expect an audible signal that initiates the trial and that the animal should not try to press the lever until after the signal. The third area that needs to be improved is to limit the movement to a single part of the animal such as the forearm. The fourth area that will be improved is to include a protocol that limits the signal to attention and expectation without motor involvement.

In order to achieve these three objectives, the following experiment is proposed. The rat will be suspended from a sling thus limiting the motion of the animal and preventing the movement around the cage. The lever arm will be positioned under the rat's arm such that it supports the arm at a 90^{o} angle at the joint of the elbow thus limiting the joint movements to the elbow and the wrist. In the first stage of the experiment, the lever and arm movement will be isometric limiting the proprioceptive sensory signals from the joint movements. This will not eliminate the sensory information entirely as there still be cutaneous activation from contact with the lever but it will limit the sensory output. An audible signal will sound initiating the start of the trial. The rat will be trained if they exert a force on the lever over a certain force threshold then the system

will not give out a reward. In this experiment the reward will be a water reward that will be released from a nozzle at the rat's mouth that they will be able to lick. This will eliminate the need for the rat to move to the food tray and introducing further contamination to the signal. The second experiment will be the same as the first in all parts however, the lever and arm movement will not be isometric but rather have spring and damping force that will allow the lever to move with a certain amount of force.

A third experiment, will be the same as the first however, there will be no lever. In this experiment the rat will be suspended in a sling. An audible signal will sound 500ms before a reward is administered. After the 500ms a liquid reward will be administered to the rat. The rat will be trained such that if they move within 500ms they will not receive the reward. This experiment will eliminate the sensory and motor components for the signal and just leave the expectation and attention aspects of the signal.

One flaw with the experiment, was that the field potentials were compared to broad motor activity in the lever press task. It was difficult to isolate certain muscle groups. One way to improve this would be to record the EMG from select muscle groups and compare the field potential data to the timings of activation of these muscle groups. This addition to the experimental set up will accomplish two things; first it will limit the comparison to certain muscle group activation, second it will allow for the separation of the sensory and motor based on the exact timing of the motor inputs. Preliminary trials have already been tried in this project, and while no results were obtained, the preliminary trials do demonstrate that the method is feasible with the current experimental setup. The implant of the electrodes into the arm showed no reduction of

the animal to perform the lever press task and the animal showed no noticeable changes in motor strategies if given a week to heal from the surgery. In other projects this method has been implemented and have obtained EMG data from the arm so the recording and implant techniques used are viable.

In order to understand the high frequency field potentials better and what function they may have in the cerebellum, the source of the signal need to be determined. To do this, a laminar penetration electrode array will be used to record from various depths of the cerebellum. The electrode will be setup such that the electrode shanks themselves are set up in an array thus giving a three dimensional view of the field potentials of the cerebellum. A stereotaxic frame will be used and the depth of the electrode will be precisely measured so that the exact depth of each electrode can be determined and the cellular layer with which it best corresponds. The primary cellular source of the high frequency potentials can be determined by the depth of the highest amplitude signal. If further refinement is needed current source density analysis can be employed. The high frequency field potentials will also be correlated to spiking recorded from each electrode. The spike type, form, and characteristics will be used to determine the cellular source that the spiking activity is coming from. This will further enable the determination of the cellular source of the high frequency potentials.

The preliminary data in this study showed that stimulation of the motor cortex in the theta band (4-9Hz) frequencies produced modulation of the high frequency potential amplitude with a peak amplitude at 7Hz. This matched with the synchrony analysis data which showed high synchrony in the same frequency range. The synchrony data also showed high synchrony regions in the Mu (10-14Hz) and Beta (15-30Hz) frequency

bands. Therefore, the stimulation analysis should be expanded to include frequencies ranging from 3-30Hz to determine if there are more than one resonance peaks.

CHAPTER 4
OTHER STUDIES

4.1 Evolution of Behavioral task

The first motor paradigm that was used in the analysis was that of face cleaning. This task had several advantages that led to its being used in the analysis. The most prominent was that this task was a natural movement that was performed often by the rat. This was beneficial in that the task required no training time. The task also required no motivation so the rat did not have to be kept on a fasting regiment that would have to be maintained and may cause discomfort to the animal. The primary problem of this method was that it was a highly learned task that has been performed by the rat since a very young age. These type of highly learned tasks do not tend to involve the cerebellum to a high degree. Another area that presented a problem was the inconsistency with which the animal performed the task. This inconsistency was due to the animal having no cue from the researchers but rather seeking its own goal in cleaning. It was also difficult to determine the state of the animal during the cleaning task. The final reason this task was less than ideal was that the cleaning activated a large amount of sensory signals in the forearm and whiskers both of which project to the area of the paramedian lobule that was being recorded from. No consistent activation of the cerebellum was determined by comparing the kinematic variables with the cerebellar activation.

The second task attempted was the food reaching task where a pellet was placed just outside the cage and the rat had to reach through a small window through the cage.

This task required a period of training and food restriction placed on the rat however, produced more stereotypical movements. The timing of the movement could also be controlled to a certain degree by the researcher by the timing of the placement of the food pellet. The state of the animal was also more certain given that the animal was performing a goal directed movement. The problem of large sensory recruitment was also diminished because the animal was not rubbing across the face. The primary problem with this method was found to be that the reaching produced no resistance on the rats and the fine movements involved in the reaching and grasping were too fast to be picked up in the video equipment used in the lab at that time and no consistent activation of the cerebellum was observed for the large scale movements that were visible.

The next motor paradigm was using resistance on the food to create more feedback and to lengthen the movement time. This task consisted of having a cereal placed in a clip that the rat had to pull out. The clip provided enough resistance that the rat was not able to quickly pull the cereal out but not so much that it was impossible. The major problem with this task was that there was a large amount of slippage between the paw and the cereal. This produced the problem of inconsistencies in the movement between trials and it also produced a large amount of sensory contamination in the signal from the paw brushing. This may have been improved by adjusting the pressure that was applied to the cereal or using other reaching tasks however, at this time the haptic lever had been developed for another project so it was not necessary.

The task used in this project was the lever press task. In this motor paradigm the rat presses a lever that is attached to a robot which provides haptic feedback. The trial period is initiated with a beep and the raising of the lever. The rat then has 10s to push

the lever for a food reward. A constant spring force and viscosity are applied to the lever through the haptic robot. After initial trials a force sensor was added to the lever to have a better judge of the timing of the movement and instantaneous force that the rat applied. This method required a significant amount of training consisting of approximately 1-2 weeks depending of the activity level of the rat. The major benefit of this method was the sensory input was limited while the movement was a long lasting movement. This, however, did not completely eliminate the contamination of the signal from sensory input and it was still major factor. The major drawback of this method was that the animal could use its body weight to push the lever therefore, complicating the analysis. Several methods for improvement of this method have been given in the Further Studies section.

4.2 Evolution of Electrode Design and Setup

The initial design of the electrode package used a 32-channel surface multi- electrode array from Multichannel Systems. The electrode layout was set up in a 6X6 array with reference electrodes on either side of the array. This electrode required a compression connector to connect to the contact pads on the electrode. Wires were then attached to the compression connector and were soldered to an Omnetics micro connector. The wires were covered in silicone to prevent them from being broken as the rat moved. The Omnetics connector was placed on the rat's skull and the compression connector was placed above the spinal cord where it was tied to a muscle. The electrode was then placed on the cerebellum extending out from the connector on the back. This technique produced a large amount of pull and torque on the electrode, causing it to break or become unattached. This reduced the life span of the electrode.

In order to prevent the pulling out and breaking of the electrode the connector needed to be removed from the back. For this reason the electrode connection was redesigned creating a printed circuit board that would connect the electrode and the Omnetics connector onto one board. The printed circuit board was designed such that one end had pads that matched the electrode connector pads. The other end had pads that matched the Omnetics connector pinout organization. The connecting leads were organized such that the corresponding electrode number matched the numbering on the Omnetics connector. The Omnetics connector was soldered onto the printed circuit board. The electrode was placed on the pads on the circuit board and soldered on. A piece of plastic was then placed over the electrode and placed in a vice pinning the electrode further to the circuit board. Epoxy was then placed over the circuit board and plastic pinning the electrode down. The connector was then placed on the skull of the rat and the electrode was run from the top of the skull to the cerebellum. This process reduced the number of failed electrodes and lengthened the time that an animal could be recorded for. The problem with this design was that the connection between the electrode and the circuit board was not consistent and some channels would be lost due to bad connections.

The Multichannel Systems electrode had some drawbacks too. The primary problem with the electrode was that it was wider than the paramedian lobule, thus the some of the electrodes were either recording nothing or recording from neighboring lobules. Another problem was that the electrode was not long enough to cover the length of the paramedian lobule to cover the zone expressing the forearm. A final flaw was that the large reference pads were not well enough secured to the polyimide and regularly

became unattached and broke. For this reason a custom built electrode was designed and built by NeuroNexus. This electrode is the current 4X8 array that was used in the projects described in the previous sections. The advantages of this electrode besides the better coverage was that the electrode come pre-attached to the Omnetics connector eliminating the work needed to assemble the electrode. Another advantage was that the electrode assembly was smaller and thus allowed for more than one electrode to be placed on the skull enabling the addition of the electrode for the motor cortex.

4.3 Animal Change

Sprague Dawley rats were initially used as the animal model for the experiments. This was due to the initial experiments being acute. As the experiments moved to chronic behavioral experiments the Sprague Dawley rat was kept to maintain consistency between the acute and chronic studies. The initial chronic studies were using face cleaning as the movement being analyzed and therefore, did not require any training. When the behavioral task was switched to the lever pressing it was observed that the Sprague Dawley rats were taking a long time to train. The Long Evans rats were used in another study in the lab and it was observed that the Long Evans rats learned at a much higher rate. It was observed that the Long Evans rats were more active than the Sprague Dawley rats and that they explored the cage to a high degree and for longer periods of time. This was crucial for the training as the training regimen required the rats to explore the cage and discover the lever several times before they learned that pushing the lever led to a food reward. In order to shorten the training times the animal model was therefore, switched to Long Evans rats.

4.4 Cerebellar Brain Computer Interface Design and Testing

One of the original goals of this project was to create a brain machine interface using the cerebellum. The rationale behind this was that the cerebellum may provide a better signal for brain machine interfacing due to the large and varied number of inputs. These inputs come from the somatosensory and motor cortices along with the frontal executive function areas. These varied inputs were thought to be able to give a more complete outlook on the motor processing than just recording from a single area of the cerebral cortex.

The task used to analyze was the face cleaning task. The animal was videotaped while performing face cleaning. The joints were marked using Matlab and the joint angles and kinematic variables were calculated. The kinematic data was then low pass filtered to a frequency range around 12Hz to eliminate artifacts from jitter of the joint location marking. The three variables of angular position, velocity, and acceleration were compared to the field potential data.

Several methods were used to parse out the relevant data from the field potentials. The first method was a simple band pass filtering to certain frequencies. The high frequencies were rectified and averaged to bring them to the correct frequency range. Both specific and multiple frequency ranges were used in the comparison. The second method of separating the signal was to separate the signal into its principle components.

The components were then rectified averaged. The third method was to use a wavelet function to separate the signal.

The parsed signals were then trained on multiple trials of kinematic data. The three variables of kinematics were compared separately and combined in multiple percentages for each variable. Linear regression was used to fit the parsed field potential data to the kinematic data. After the data was trained on the training trials the coefficients for each channel or component of the signal were then applied to a series of test trials to determine the overall fit of the function. The R^2 value was then used to determine how well the data fit to the kinematic data.

These methods were applied to both the cerebellum and the primary motor cortex. The primary motor cortex was used as a gold standard test since it is the most common area used to drive current brain computer interface systems. The R^2 value for both were calculated and the cerebellar performance was compared to the primary motor cortex. The goal of this project was to demonstrate that the cerebellum performed better than the motor cortex at predicting the kinematic variables. After a large number of attempts to demonstrate this, the project was abandoned to pursue the current research.

APENDEX A

SYNCHRONY ANALYSIS CODE

For phase synchrony we developed our own Matlab code based on the analysis method described in (Tass, Rosenblum et al. 1998). In brief, the phase information in each neural channel was found from the analytic signal of the Hilbert transformation as a function of time in a running window. Shannon entropy was computed and used as a synchrony measure from the statistics of inter-channel synchrony given the assumption that two signals are synchronous for a given time window when their differential phase is approximately constant.

```
clear all
sampling_rate=20000;
 positions= [8 16 6 14 4 12 2 10 1 9 3 11 5 13 7 15 31 23 29 21 27 19 25 17 26 18 28 20
30 22 24];
 win=2000;
 N=round(exp(0.626+0.4*log(win-1)));
 H_max=log(N);

  f1=2;
f2=2;

  for r=1:30
        runs=200;
        fc1=f1+(r-1);
        fc2=f2+(r-1);
        fn2=2*fc2/(sampling_rate);
        fn1=2*fc1/(sampling_rate);
 for u=1:runs
```

```
    data1=randn(win+1,1);
    data2=randn(win+1,1);



        [b,a]=butter(4,fn2,'low');
        fdata1=filtfilt(b,a,data1);
        [b,a]=butter(4,fn1,'high');
        fdata1=filtfilt(b,a,fdata1);



        [b,a]=butter(4,fn2,'low');
        fdata2=filtfilt(b,a,data2);
        [b,a]=butter(4,fn1,'high');
        fdata2=filtfilt(b,a,fdata2);

    H1=hilbert(fdata1);
    H2=hilbert(fdata2);
    A_H1=unwrap(angle(H1));
    A_H2=unwrap(angle(H2));
    ds=A_H1-A_H2;
    y=hist(ds,N)/win;
y(y==0)=0.00000001;
  H_s=abs(sum((y).*log(y)));
gamma_test(u)=(H_max-H_s)/H_max;
 end
  end


 for j=1:31
    j
 trialnums=[3 4 5 8 10 12 13 14 15 16 19 20 21 22 24 25 26 27 28 29 31 35 36 37 40 42
44 47 53 54 55 56 59 60 61 65 67 68 70 72 73 74];
times=[1 3.8 2.6 2.8 1 3.6 4 2.5 1.8 2.9 4.7 1.5 1.1 1.4 1.9 1.7 2.4 3.7 3.6 1.9 3.2 1.5 2.1
2.1 2.0 1.4 2.7 1.5 1.2 2.3 1.8 1 1.6 1.9 1 1.8 2.5 2.3 2.7 2.7 2.3 1.5 3.1];
```

```
times=(times+0.442).*20000;
% times=(times+0.442).*20000;
 positions= [8 16 6 14 4 12 2 10 1 9 3 11 5 13 7 15 31 23 29 21 27 19 25 17 26 18 28 20
30 22 24];

parfor m=1:length(trialnums)

    trial=trialnums(m);
    file_name = ['trial' num2str(trial) ];     % user insert appropriate file name
% num2str(trial)
raw_data_cerebellum = daqread(['data\raw_daq\' file_name 'B' '.daq']);
raw_data_cortex=daqread(['data\raw_daq\' file_name 'A' '.daq']);
unfiltered_data_name = ['data\unfiltered\' file_name '.dat'];
filtered_data_name = ['data\filtered\' file_name '.dat'];
envelope_name = ['data\envelope\' file_name '.dat'];

% Set the recording parameters according to what was used for signal
% acquisition.

number_channels =31;
amplifier_gain = 100;
sampling_rate = 20000;  % in samples/sec
video_frame_rate = 30;  % in frames/sec

 unfiltered_data_cerebellum = detrend(raw_data_cerebellum/amplifier_gain);
  unfiltered_data_cortex = detrend(raw_data_cortex/amplifier_gain);



  unfiltered_data_cerebellum=unfiltered_data_cerebellum(:,:);
  unfiltered_data_cortex=unfiltered_data_cortex(:,:);

%   [coef, score, latent]=princomp(unfiltered_data_cerebellum);

% coef(:,1)=zeros(number_channels,1);
%   coef(:,2)=zeros(number_channels,1);
```

```
%  coef(:,3)=zeros(number_channels,1);
% unfiltered_data_cerebellum=score*coef';

f1=2;
f2=2;

 for r=1:30
        runs=200;
        fc1=f1+(r-1);
        fc2=f2+(r-1);
        fn2=2*fc2/(sampling_rate);
        fn1=2*fc1/(sampling_rate);
%  for u=1:runs
%     data1=randn(win+1,1);
%     data2=randn(win+1,1);
%
%
%
%           [b,a]=butter(4,fn2,'low');
%           fdata1=filtfilt(b,a,data1);
%           [b,a]=butter(4,fn1,'high');
%           fdata1=filtfilt(b,a,fdata1);
%
%
%
%           [b,a]=butter(4,fn2,'low');
%           fdata2=filtfilt(b,a,data2);
%           [b,a]=butter(4,fn1,'high');
%           fdata2=filtfilt(b,a,fdata2);
%
%     H1=hilbert(fdata1);
%     H2=hilbert(fdata2);
%     A_H1=unwrap(angle(H1));
%     A_H2=unwrap(angle(H2));
```

```
%      ds=A_H1-A_H2;
%      y=hist(ds,N)/win;
% y(y==0)=0.00000001;
%   H_s=abs(sum((y).*log(y)));
% gamma_test(u)=(H_max-H_s)/H_max;
%  end



          [b,a]=butter(4,fn2,'low');
          LFP_data=filtfilt(b,a,unfiltered_data_cerebellum);
          [b,a]=butter(4,fn1,'high');
          LFP_data=filtfilt(b,a,LFP_data);

%             [b,a]=butter(4,fn2,'low');
%             LFP_data2=filtfilt(b,a,unfiltered_data_cerebellum);
%             [b,a]=butter(4,fn1,'high');
%             LFP_data2=filtfilt(b,a,LFP_data);

 for h=1:30
   t= (times(m)-15000)+(h-1)*1000;
   H=hilbert(LFP_data(t:t+win,1:31));
%     H_c=hilbert(LFP_data2(t:t+win,1:31));
%   H=hilbert(LFP_data(:,1:31));

A_H=unwrap(angle(H));
% A_H_c=unwrap(angle(H_c));

for i=1:31
ds=A_H(:,j)-A_H(:,i);
% ds=A_H_c(:,j)-A_H(:,i);

y=hist(ds,N)/win;
% clear ds
```

```
y(y==0)=0.00000001;
  H_s=abs(sum((y).*log(y)));
%   clear y
g=(H_max-H_s)/H_max;
% clear H_s
test=gamma_test;
test(test<g)=0;
test(test>=g)=1;
p=sum(test)/runs;
if p<=0.05
    gamma(m,h,r,i)=g;
else
    gamma(m,h,r,i)=0;
end
% clear g
end

% figure; plot(der)
 end
  end
end
% mean_gamma=mean(gamma);
% %figure; plot(A_H)
% figure;
%  for k=1:31
% subplot(4,8,positions(k))
% contourf(squeeze(mean_gamma(:,:,:,k))')
% caxis([0 .3])
%  end
 name=['leverpress_low_2_32_longer_12trial_chan' num2str(j) '.mat'];
save(name, 'gamma')
%  figure; surface(squeeze(mean_gamma)')
%  figure; contourf(squeeze(mean_gamma)')
 end
```

APENDEX B

CLUSTERING ANALYSIS CODE

Clustering analysis was performed on the inter-contact synchrony values to determine which channels followed a similar trend as a group around the time of lever press and if there was a spatial pattern to the synchrony. The synchrony values were averaged across the frequency band of interest (150-350Hz) between all contact pairs during lever press in multiple trials. A long vector was formed for each contact that consisted of its synchrony values with all the other contacts as a function of time (11 time points at 50 ms intervals) and in multiple trials. In other words, each vector contained many small vectors of 11 synchrony values, concatenated with other small vectors resulting from multiple trials and with multiple contacts. This way all the variation across the trials was contained in one large vector by combining the inter-contact synchrony data from all trials. The synchrony vectors from all 31 contacts were then clustered using the k-means method in Matlab. Since the clusters were observed to change between clustering attempts, one thousand clustering iterations were implemented with randomized starting points. This accounted for the variations in clustering due to the dependency of the algorithm on the starting points. The success rates of clustering together were calculated between each contact pair. Contact pairs that ended up in the same cluster in greater than or equal to 95% of the attempt were considered to be in the same group. After the final groups were derived, the centroids of the contact groups (i.e. their vectors) and Euclidian distances from the centroid to each vector were calculated. The strength of membership for each contact to a group was calculated using the following equation.

```
index=1;
for i=1:31
% name=['leverpress_high_250_350_longer_chan' num2str(i) '.mat'];
 name=['leverpress_high_250_350_longer_12trial_chan' num2str(i) '.mat'];
%  name=['CeC0phasesynch_low_chan' num2str(i) '.mat'];
load(name)
x=size(gamma);

for j=1:x(1)
   for k=1:31
mean_synchs(k,index:index+10)=mean(squeeze(gamma(j,10:20,:,k))');
   end
 index=index+11;
end
% for j=1:x(1)
%     for k=1:31
% mean_synchs(k,index)=mean(mean(squeeze(gamma(j,10:20,:,k))'));
%     end
%  index=index+1;
% end
end
% sumdn=zeros(5,1000);
for rep=1:1000
n=3;
[idxs,C,sumd,D]= kmeans(mean_synchs,n);
Dn(:,:,rep)=D;
  sumdn(:,rep)=sumd;
idx(:,rep)=idxs;

end
rep=1000;
for i=1:31
   for j=1:31
```

```
        for r=1:rep
            if idx(i,r)==idx(j,r)
                y(r)=1;
            else
                y(r)=0;
            end
            c=sum(y)/rep;
            if ge(c,.95)
                cluster_P(i,j)=1;
            else
                cluster_P(i,j)=0;
            end
        end
    end
end
save('cluster_P.mat', 'cluster_P')
figure; surface(cluster_P)

for i=1:31
    for j=1:1000
        sumdx(i,j)=sumdn(idx(i,j),j);
    end
end



for i=1:31
    for j=1:1000
        Dx(i,j)=Dn(i,idx(i,j),j);
    end
end
% n=5
%
% [IDX,C,sumd,D]= kmeans(cluster_P,n,'emptyaction','drop');
 positions= [16 14 12 10 9 11 13 15 23 21 19 17 18 20 22 24 8 6 4 2 1 3 5 7 31 29 27 25
26 28 30 32];
```

```
%   positions= [8 16 6 14 4 12 2 10 1 9 3 11 5 13 7 15 31 23 29 21 27 19 25 17 26 18 28
20 30 22 24];
%  figure
%  for k=1:31
% subplot(4,8,positions(k))
% surface(ones(2,2).*IDX(k))
% % contourf(squeeze(mean_gamma(:,:,1:15,31))')
% % contourf(squeeze(gamma(1,:,1:30,k))')
%  caxis([1 n])
%  end

 for j=1:31
     figure
  for k=1:31
subplot(4,8,positions(k))
surface(ones(2,2).*cluster_P(j,k))
% contourf(squeeze(mean_gamma(:,:,1:15,31))')
% contourf(squeeze(gamma(1,:,1:30,k))')
 caxis([0 1])
  end
 end

 for i=1:50
     figure
[silh4,h] = silhouette(mean_synchs,idx(:,i));
set(get(gca,'Children'),'FaceColor',[.8 .8 1])
xlabel('Silhouette Value')
ylabel('Cluster')
end
```

REFERENCES

Adrian, E. D. (1934). "Discharge Frequencies in the Cerebral and Cerebellar Cortex." Proceedings of the Physiological Society: 32-33.

Adrian, E. D. (1943). "Afferent areas in the cerebellum connected with the limbs." Brain 66(4): 289-315.

Allen, G. I., G. B. Azzena and T. Ohno (1972). "Contribution of the cerebro-reticulo-cerebellar pathway to the early mossy fibre response in the cerebellar cortex." Brain Research 44(2): 670-675.

Anderson, R. F. (1943). "Cerebellar distribution of the dorsal and ventral spino-cerebellar tracts." The Journal of Comparative Neurology 79(3): 415-423.

Andersson, G. and J. Nyquist (1983). "Origin and sagittal termination areas of cerebro-cerebellar climbing fibre paths in the cat." The Journal of Physiology 337(1): 257-285.

Andersson, G. and O. Oscarsson (1978). "Climbing fiber microzones in cerebellar vermis and their projection to different groups of cells in the lateral vestibular nucleus." Exp Brain Res 32(4): 565-579.

Apps, R. and M. Garwicz (2005). "Anatomical and physiological foundations of cerebellar information processing." Nature Reviews Neuroscience 6(4): 297-311.

Apps, R. and R. Hawkes (2009). "Cerebellar cortical organization: A one-map hypothesis." Nature Reviews Neuroscience 10(9): 670-681.

Armstrong, D. M. and T. Drew (1980). "Responses in the posterior lobe of the rat cerebellum to electrical stimulation of cutaneous afferents to the snout." Journal of Physiology VOL.309: 357-374.

Armstrong, D. M. and R. J. Harvey (1968). "Responses of a spino-olivo-cerebellar pathway in the cat." The Journal of Physiology 194(1): 147-168.

Armstrong, D. M., R. J. Harvey and R. F. Schild (1971). "Climbing fibre pathways from the forelimbs to the paramedian lobule of the cerebellum." Brain Research 25(1): 199-202.

Bell, C. C. and R. J. Grimm (1969). “Discharge properties of Purkinje cells recorded on single and double microelectrodes.” Journal of Neurophysiology 32(6): 1044-1055.

Benchenane, K., P. H. Tiesinga and F. P. Battaglia (2011). "Oscillations in the prefrontal cortex: a gateway to memory and attention." Current Opinion in Neurobiology 21(3): 475-485.

Bengtsson, F. and H. Jörntell (2007). "Ketamine and xylazine depress sensory-evoked parallel fiber and climbing fiber responses." Journal of Neurophysiology 98(3): 1697-1705.

Bokil, H., P. Andrews, J. E. Kulkarni, S. Mehta and P. P. Mitra (2010). "Chronux: A platform for analyzing neural signals." Journal of Neuroscience Methods 192(1): 146-151.

Bower, J. M., D. H. Beermann, J. M. Gibson, G. M. Shambes and W. Welker (1981). "Principles of Organization of a Cerebro-Cerebellar Circuit." Brain, Behavior and Evolution 18(1-2): 1-18.

Brodal, P. (1978). “The corticopontine projection in the rhesus monkey. Origin and principles of organization.” Brain 101(2): 251-283

Buisseret-Delmas, C. and P. Angaut (1993). "The cerebellar olivo-corticonuclear connections in the rat." Progress in Neurobiology 40(1): 63-87.

Buzsaki, G. (2006). Rhythms of the Brain, New York, Oxford University Press.

Buzsáki, G. and A. Draguhn (2004). "Neuronal olscillations in cortical networks." Science 304(5679): 1926-1929.

Cerminara, N. L., et al. (2013). "Structural basis of cerebellar microcircuits in the rat." Journal of Neuroscience 33(42): 16427-16442.

Cheron, G., et al. (2008). "Cerebellar network plasticity: From genes to fast oscillation." Neuroscience 153(1): 1-19.

Cheron, G., et al. (2004). “Fast oscillation in the cerebellar cortex of calcium binding protein-deficient mice: A new sensorimotor arrest rhythm. Prog Brain Res.” 148: 167-180.

Chorev, E., Y. Yarom and I. Lampl (2007). "Rhythmic episodes of subthreshold membrane potential oscillations in the rat inferior olive nuclei in vivo." Journal of Neuroscience 27(19): 5043-5052.

Courtemanche, R., P. Chabaud and Y. Lamarre (2009). "Synchronization in primate cerebellar granule cell layer local field potentials: Basic anisotropy and dynamic changes during active expectancy." Frontiers in Cellular Neuroscience 3: 6.

Courtemanche, R. and Y. Lamarre (2005). "Local field potential oscillations in primate cerebellar cortex: Synchronization with cerebral cortex during active and passive expectancy." Journal of Neurophysiology 93(4): 2039-2052.

Courtemanche, R., J. P. Pellerin and Y. Lamarre (2002). "Local field potential oscillations in primate cerebellar cortex: Modulation during active and passive expectancy." Journal of Neurophysiology 88(2): 771-782.

D'Angelo, E. (2008). "The Critical Role of Golgi Cells in Regulating Spatio-Temporal Integration and Plasticity at the Cerebellum Input Stage." Frontiers in Neuroscience 2(1): 35-46.

D'Angelo, E., S. K. E. Koekkoek, P. Lombardo, S. Solinas, E. Ros, J. Garrido, M. Schonewille and C. I. De Zeeuw (2009). "Timing in the cerebellum: oscillations and resonance in the granular layer." Neuroscience 162(3): 805-815.

D'Angelo, E., T. Nieus, A. Maffei, S. Armano, P. Rossi, V. Taglietti, A. Fontana and G. Naldi (2001). "Theta-frequency bursting and resonance in cerebellar granule cells: Experimental evidence and modeling of a slow K+-dependent mechanism." Journal of Neuroscience 21(3): 759-770.

D'Angelo, E., S. Solinas, J. Mapelli, D. Gandolfi, L. Mapelli and F. Prestori (2013). "The cerebellar Golgi cell and spatiotemporal organization of granular layer activity." Frontiers in Neural Circuits 17(7): 93.

D'Angelo, E. and C. I. De Zeeuw (2009). "Timing and plasticity in the cerebellum: focus on the granular layer." Trends in Neurosciences 32(1): 30-40.

Dalal, S. S., et al. (2013). "Oscillatory activity of the human cerebellum: The intracranial electrocerebellogram revisited." Neuroscience and Biobehavioral Reviews 37(4): 585-593.

De Montigny, C. and Y. Lamarre (1973). "Rhythmic activity induced by harmaline in the olivo-cerebello-bulbar system of the cat." Brain Research 53(1): 81-95.

Devor, A. and Y. Yarom (2002). "Generation and propagation of subthreshold waves in a network of inferior olivary neurons." Journal of Neurophysiology 87(6): 3059-3069.

de Solages, C., et al. (2008). "High-frequency organization and synchrony of activity in the purkinje cell layer of the cerebellum." Neuron 58(5): 775-788.

De Zeeuw, C. I., et al. (2011). "Spatiotemporal firing patterns in the cerebellum." Nature Reviews Neuroscience 12(6): 327-344.

Díez-García, J., W. Akemann and T. Knöpfel (2007). "In vivo calcium imaging from genetically specified target cells in mouse cerebellum." NeuroImage 34(3): 859-869.

Donoghue, J. P., J. N. Sanes, N. G. Hatsopoulos and G. Gaál (1998). “Neural discharge and local field potential oscillations in primate motor cortex during voluntary movements.” Journal of Neurophysiology 79(1): 159-73.

Ebner, T. J., A. L. Hewitt and L. S. Popa (2011). "What features of limb movements are encoded in the discharge of cerebellar neurons?" Cerebellum 10(4): 683-693.

Eccles, J. C., K. Sasaki and P. Strata (1967). "Interpretation of the potential fields generated in the cerebellar cortex by a mossy fibre volley." Experimental Brain Research 3(1): 58-80.

Garwicz, M., et al. (1998). "Organizational Principles of Cerebellar Neuronal Circuitry." News Physiological Science 13: 26-32.

Garwicz, M., et al. (1998). "Cutaneous receptive fields and topography of mossy fibres and climbing fibres projecting to cat cerebellar C3 zone." J Physiology 512 (1): 277-293.

Hartmann, M. J. and J. M. Bower (1998). "Oscillatory activity in the cerebellar hemispheres of unrestrained rats." Journal of Neurophysiology 80(3): 1598-1604.

Heck, D. H., W. T. Thach and J. G. Keating (2007). "On-beam synchrony in the cerebellum as the mechanism for the timing and coordination of movement." Proceedings of the National Academy of Sciences of the United States of America 104(18): 7658-7663.

Hewitt, A. L., L. S. Popa, S. Pasalar, C. M. Hendrix and T. J. Ebner (2011). "Representation of limb kinematics in Purkinje cell simple spike discharge is conserved across multiple tasks." Journal of Neurophysiology 106(5): 2232-2247.

Higuchi, S., H. Imamizu and M. Kawato (2007). "Cerebellar activity evoked by common tool-use execution and imagery tasks: an fMRI study." Cortex 43(3): 350-358.

Hirano, T. (2006). "Motor control mechanism by the cerebellum [1]." Cerebellum 5(4): 296.

Hirono, M. and K. Obata (2006). "Alpha-adrenoceptive dual modulation of inhibitory GABAergic inputs to Purkinje cells in the mouse cerebellum." J Neurophysiol 95(2): 700-708.

Houk, J. C. and S. P. Wise (1995). "Distributed modular architectures linking basal ganglia, cerebellum, and cerebral cortex: Their role in planning and controlling action." Cerebral Cortex 5(2): 95-110.

Huang, C.-m., L. Wang and R. H. Huang (2006). "Cerebellar granule cell: ascending axon and parallel fiber." European Journal of Neuroscience 23(7): 1731-1737.

Hulsmann, E., M. Erb and W. Grodd (2003). "From will to action: sequential cerebellar contributions to voluntary movement." Neuroimage 20(3): 1485-1492.

Isope, P., et al. (2002). “Temporal organization of activity in the cerebellar cortex: A manifesto for synchrony.” Ann N Y Acad Sci. 978: 164-174.

Ito, M. (2010). Cerebellar Microcircuitry. Encyclopedia of Neuroscience: 723-728.

Javalkar, V., R. E. Kelley, E. Gonzalez-Toledo, J. McGee and A. Minagar (2014). "Acute ataxias: Differential diagnosis and treatment approach." Neurologic Clinics 32(4): 881-891.

Jensen, O., P. Goel, N. Kopell, M. Pohja, R. Hari and B. Ermentrout (2005). "On the human sensorimotor-cortex beta rhythm: Sources and modeling." NeuroImage 26(2): 347-355.

Kawato, M. (1993). “Inverse dynamics model in the cerebellum.” Proceedings of the International Joint Conference on Neural Networks.

Kawato, M. and H. Gomi (1992). "A computational model of four regions of the cerebellum based on feedback-error learning." Biological Cybernetics 68(2): 95-103.

Kettner, R. E., S. Mahamud, H. C. Leung, N. Sitkoff, J. C. Houk, B. W. Peterson and A. G. Barto (1997). "Prediction of complex two-dimensional trajectories by a cerebellar model of smooth pursuit eye movement." Journal of Neurophysiology 77(4): 2115-2130.

Lamarre, Y., C. de Montigny, M. Dumont and M. Weiss (1971). "Harmaline-induced rhythmic activity of cerebellar and lower brain stem neurons." Brain Research 32(1): 246-250.

Lang, E. J., I. Sugihara, J. P. Welsh and R. Llinás (1999). "Patterns of spontaneous purkinje cell complex spike activity in the awake rat." Journal of Neuroscience 19(7): 2728-2739.

Lee, H., G. V. Simpson, N. K. Logothetis and G. Rainer (2005). "Phase Locking of Single Neuron Activity to Theta Oscillations during Working Memory in Monkey Extrastriate Visual Cortex." Neuron 45(1): 147-156.

Leznik, E., V. Makarenko and R. Llinás (2002). "Electrotonically Mediated Oscillatory Patterns in Neuronal Ensembles: An in Vitro Voltage-Dependent Dye-Imaging Study in the Inferior Olive." Journal of Neuroscience 22(7): 2804-2815.

Llinas, R., R. Baker and C. Sotelo (1974). "Electrotonic coupling between neurons in cat inferior olive." Journal of Neurophysiology 37(3): 560-571.

Lotze, M., P. Montoya, M. Erb, E. Hülsmann, H. Flor, U. Klose, N. Birbaumer and W. Grodd (1999). "Activation of Cortical and Cerebellar Motor Areas during Executed and Imagined Hand Movements: An fMRI Study." Journal of Cognitive Neuroscience 11(5): 491-501.

Lu, H., M. J. Hartmann and J. M. Bower (2005). "Correlations between purkinje cell single-unit activity and simultaneously recorded field potentials in the immediately underlying granule cell layer." Journal of Neurophysiology 94(3): 1849-1860.

Lundberg, A. and O. Oscarsson (1960). "Functional Organization of the Dorsal Spino-Cerebellar Tract in the Cat." Acta Physiologica Scandinavica 50(3-4): 356-374.

Manto, M. and A. J. Bastian (2007). "Cerebellum and the deciphering of motor coding." Cerebellum 6(1): 3-6.

Middleton, S. J., et al. (2008). "High-Frequency Network Oscillations in Cerebellar Cortex." Neuron 58(5): 763-774.

Mizuno, N., K. Mochizuki, C. A. R. Matsushima and K. Sasaki (1973). "Projections from the parietal cortex to the brain stem nuclei in the cat, with special reference to the parietal cerebro-cerebellar system." The Journal of Comparative Neurology 147(4): 511-521.

Murthy, V. N. and E. E. Fetz (1992). "Coherent 25- to 35-Hz oscillations in the sensorimotor cortex of awake behaving monkeys." Proceedings of the National Academy of Sciences 89(12): 5670-5674.

Nowak, D. A., H. Topka, D. Timmann, H. Boecker and J. Hermsdörfer (2007). "The role of the cerebellum for predictive control of grasping." Cerebellum 6(1): 7-17.

O'Connor, S. M., R. W. Berg and D. Kleinfeld (2002). Coherent Electrical Activity Between Vibrissa Sensory Areas of Cerebellum and Neocortex Is Enhanced During Free Whisking.

Oehler, J., et al. (1969). "The bioelectrical activity of cerebellar structures in the freely-moving rat." Conditional reflex : a Pavlovian journal of research & therapy 4(3): 187-198.

Odeh, F., R. Ackerley, J. G. Bjaalie and R. Apps (2005). "Pontine maps linking somatosensory and cerebellar cortices are in register with climbing fiber somatotopy." Journal of Neuroscience 25(24): 5680-5690.

Ordek, G., J. D. Groth and M. Sahin (2013). "Differential effects of ketamine/xylazine anesthesia on the cerebral and cerebellar cortical activities in the rat." Journal of Neurophysiology 109(5): 1435-1443.

Pellerin, J. P. and Y. Lamarre (1997). "Local field potential oscillations in primate cerebellar cortex during voluntary movement." Journal of Neurophysiology 78(6): 3502-3507.

Pesaran, B., J. S. Pezaris, M. Sahani, P. P. Mitra and R. A. Andersen (2002). "Temporal structure in neuronal activity during working memory in macaque parietal cortex." Nature Neuroscience 5(8): 805-811.

Picazio, S., D. Veniero, V. Ponzo, C. Caltagirone, J. Gross, G. Thut and G. Koch (2014). "Prefrontal control over motor cortex cycles at beta frequency during movement inhibition." Current Biology 24(24): 2940-2945.

Popa, D., M. Spolidoro, R. D. Proville, N. Guyon, L. Belliveau and C. Léna (2013). "Functional role of the cerebellum in gamma-band synchronization of the sensory and motor cortices." Journal of Neuroscience 33(15): 6552-6556.

Ramnani, N. (2006). "The primate cortico-cerebellar system: Anatomy and function." Nature Reviews Neuroscience 7(7): 511-522.

Ronnqvist, K. C., C. J. McAllister, G. L. Woodhall, I. M. Stanford and S. D. Hall (2013). "A multimodal perspective on the composition of cortical oscillations." Frontiers in Human Neuroscience.

Roš, H., R. N. S. Sachdev, Y. Yu, N. Šestan and D. A. McCormick (2009). "Neocortical networks entrain neuronal circuits in cerebellar cortex." Journal of Neuroscience 29(33): 10309-10320.

Salmi, J., K. J. Pallesen, T. Neuvonen, E. Brattico, A. Korvenoja, O. Salonen and S. Carlson (2009). "Cognitive and Motor Loops of the Human Cerebro-cerebellar System." Journal of Cognitive Neuroscience 22(11): 2663-2676.

Sanes, J. N. and J. P. Donoghue (1993). "Oscillations in local field potentials of the primate motor cortex during voluntary movement." Proceedings of the National Academy of Sciences 90(10): 4470-4474.

Schmahmann, J. D. (2010). "The role of the cerebellum in cognition and emotion: personal reflections since 1982 on the dysmetria of thought hypothesis, and its

historical evolution from theory to therapy." Neuropsychology Review 20(3): 236-260.

Schweighofer, N. (1998). "Role of the cerebellum in reaching movements in humans. I. Distributed inverse dynamics control." European Journal of Neuroscience 10(1): 86-94.

Shadmehr, R. and J. W. Krakauer (2008). "A computational neuroanatomy for motor control." Experimental Brain Research 185(3): 359-381.

Shambes, G. M., D. H. Beermann and W. Welker (1978). "Multiple tactile areas in cerebellar cortex: another patchy cutaneous projection to granule cell columns in rats." Brain Research 157(1): 123-128.

Shambes, G. M., J. M. Gibson and W. Welker (1978). "Fractured somatotopy in granule cell tactile areas of rat cerebellar hemispheres revealed by micromapping." Brain, Behavior and Evolution 15(2): 94-140.

Shambes, G. M., J. M. Gibson and W. Welker (1978). "Fractured Somatotopy in Granule Cell Tactile Areas of Rat Cerebellar Hemispheres Revealed by Micromapping; pp. 116–140." Brain, Behavior and Evolution 15(2): 116-140.

Shepherd, G. (2004). Synaptic organization of the brain. New York, Oxford University Press.

Shidara, M., K. Kawano, H. Gomi and M. Kawato (1993). "Inverse-dynamics model eye movement control by Purkinje cells in the cerebellum." Nature 365(6441): 50-52.

Snider, R. and E. Eldred (1951). "Electro-anatomical studies on cerebro-cerebellar connections in the cat." The Journal of Comparative Neurology 95(1): 1-16.

Solinas, S., L. Forti, E. Cesana, J. Mapelli, E. De Schutter and E. D'Angelo (2007). "Computational Reconstruction of Pacemaking and Intrinsic Electroresponsiveness in Cerebellar Golgi Cells." Frontiers in Cellular Neuroscience 1: 2.

Solinas, S., L. Forti, E. Cesana, J. Mapelli, E. De Schutter and E. D'Angelo (2007). "Fast-Reset of Pacemaking and Theta-Frequency Resonance Patterns in Cerebellar Golgi Cells: Simulations of their Impact In Vivo." Frontiers in Cellular Neuroscience 1: 4.

Stosiek, C., O. Garaschuk, K. Holthoff and A. Konnerth (2003). "In vivo two-photon calcium imaging of neuronal networks." Proceedings of the National Academy of Sciences 100(12): 7319-7324.

Sugimori, M. and R. R. Llinás (1990). "Real-time imaging of calcium influx in mammalian cerebellar Purkinje cells in vitro." Proceedings of the National Academy of Sciences 87(13): 5084-5088.

Sullivan, M. R., A. Nimmerjahn, D. V. Sarkisov, F. Helmchen and S. S. Wang (2005). "In vivo calcium imaging of circuit activity in cerebellar cortex." J Neurophysiol 94(2): 1636-1644.

Sultan, F. and M. Glickstein (2007). "The cerebellum: Comparative and animal studies." Cerebellum 6(3): 168-176.

Tamada, T., S. Miyauchi, H. Imamizu, T. Yoshioka and M. Kawato (1999). "Cerebro-cerebellar functional connectivity revealed by the laterality index in tool-use learning." NeuroReport 10(2): 325-331.

Taniwaki, T., A. Okayama, T. Yoshiura, O. Togao, Y. Nakamura, T. Yamasaki, K. Ogata, H. Shigeto, Y. Ohyagi, J. i. Kira and S. Tobimatsu (2006). "Functional network of the basal ganglia and cerebellar motor loops in vivo: Different activation patterns between self-initiated and externally triggered movements." NeuroImage 31(2): 745-753.

Tank, D., M. Sugimori, J. Connor and R. Llinas (1988). "Spatially resolved calcium dynamics of mammalian Purkinje cells in cerebellar slice." Science 242(4879): 773-777.

Tass, P., M. G. Rosenblum, J. Weule, J. Kurths, A. Pikovsky, J. Volkmann, A. Schnitzler and H. J. Freund (1998). "Detection of n:m phase locking from noisy data: Application to magnetoencephalography." Physical Review Letters 81(15): 3291-3294.

Thach, W. T. (1968). "Discharge of Purkinje and cerebellar nuclear neurons during rapidly alternating arm movements in the monkey." Journal of Neurophysiology 31(5): 785-797.

Voogd, J. and M. Glickstein (1998). "The anatomy of the cerebellum." Trends in Cognitive Sciences 2(9): 307-313.

Voogd, J., et al. (1981). "Structure and fiber connections of the cerebellum." Progress in clinical and biological research 59 A: 259-268.

Voogd, J., J. Pardoe, T. J. H. Ruigrok and R. Apps (2003). "The distribution of climbing and mossy fiber collateral branches from the copula pyramidis and the paramedian lobule: Congruence of climbing fiber cortical zones and the pattern of zebrin banding within the rat cerebellum." Journal of Neuroscience 23(11): 4645-4656.

Voogd, J. and T. J. H. Ruigrok (2004). "The organization of the corticonuclear and olivocerebellar climbing fiber projections to the rat cerebellar vermis: The congruence of projection zones and the zebrin pattern." Journal of Neurocytology 33(1 SPEC. ISS.): 5-21.

Witter, L., et al. (2013). "Strength and timing of motor responses mediated by rebound firing in the cerebellar nuclei after Purkinje cell activation." Frontiers in Neural Circuits 7.